catalysts

MDPI

Article

Photocatalytic Hydrogen Production: Role of Sacrificial Reagents on the Activity of Oxide, Carbon, and Sulfide Catalysts

Vignesh Kumaravel [1,2,*], Muhammad Danyal Imam [3], Ahmed Badreldin [3], Rama Krishna Chava [4], Jeong Yeon Do [4], Misook Kang [4,*] and Ahmed Abdel-Wahab [3,*]

1 Department of Environmental Science, School of Science, Institute of Technology Sligo, Ash Lane, F91 YW50 Sligo, Ireland
2 Centre for Precision Engineering, Materials and Manufacturing Research (PEM), Institute of Technology Sligo, Ash Lane, F91 YW50 Sligo, Ireland
3 Chemical Engineering Program, Texas A&M University at Qatar, Doha 23874, Qatar; muhammad.imam@qatar.tamu.edu (M.D.I.); ahmed.badreldin@qatar.tamu.edu (A.B.)
4 Department of Chemistry, College of Natural Sciences, Yeungnam University, Gyeongsan, Gyeongbuk 38541, Korea; drcrkphysics@hotmail.com (R.K.C.); daengi77@ynu.ac.kr (J.Y.D.)
* Correspondence: Kumaravel.Vignesh@itsligo.ie (V.K.); mskang@ynu.ac.kr (M.K.); ahmed.abdel-wahab@qatar.tamu.edu (A.A.-W.)

Received: 15 February 2019; Accepted: 11 March 2019; Published: 18 March 2019

Abstract: Photocatalytic water splitting is a sustainable technology for the production of clean fuel in terms of hydrogen (H_2). In the present study, hydrogen (H_2) production efficiency of three promising photocatalysts (titania (TiO_2-P25), graphitic carbon nitride (g-C_3N_4), and cadmium sulfide (CdS)) was evaluated in detail using various sacrificial agents. The effect of most commonly used sacrificial agents in the recent years, such as methanol, ethanol, isopropanol, ethylene glycol, glycerol, lactic acid, glucose, sodium sulfide, sodium sulfite, sodium sulfide/sodium sulfite mixture, and triethanolamine, were evaluated on TiO_2-P25, g-C_3N_4, and CdS. H_2 production experiments were carried out under simulated solar light irradiation in an immersion type photo-reactor. All the experiments were performed without any noble metal co-catalyst. Moreover, photolysis experiments were executed to study the H_2 generation in the absence of a catalyst. The results were discussed specifically in terms of chemical reactions, pH of the reaction medium, hydroxyl groups, alpha hydrogen, and carbon chain length of sacrificial agents. The results revealed that glucose and glycerol are the most suitable sacrificial agents for an oxide photocatalyst. Triethanolamine is the ideal sacrificial agent for carbon and sulfide photocatalyst. A remarkable amount of H_2 was produced from the photolysis of sodium sulfide and sodium sulfide/sodium sulfite mixture without any photocatalyst. The findings of this study would be highly beneficial for the selection of sacrificial agents for a particular photocatalyst.

Keywords: photocatalysis; TiO_2; g-C_3N_4; CdS; energy

1. Introduction

Photocatalytic hydrogen (H_2) production via water splitting is a sustainable and renewable energy production technology with negligible impact on the environment [1] (Figure 1). H_2 is one of the most promising and clean energy sources for the future, with water as the only combustion product. After the invention of photo-electrochemical water splitting in 1972 [2] by Fujishima and Honda, nearly 9000 research articles have been published, outlining the use of various photocatalysts. In particular, most of the research works have been carried out using powder photocatalysts (except photo-electrochemical studies). The reported materials in the recent years are categorized as oxide

[3–149], carbon [3,81,150–237], and sulfide [3,14,17,35,58,59,113,114,119,128,133,154,164,169,177,181,195,203,208,210,215,220,227,230,235,238–345] photocatalysts. Titanium oxide–P25 (TiO_2-P25), graphitic carbon nitride (g-C_3N_4), and cadmium sulfide (CdS) are the most extensively studied photocatalysts for water splitting. Many review articles have also been published [1,116,163,167,225,237,238,245,346–419] discussing the various features of the photocatalytic water splitting, such as fundamental concepts, theoretical principles, nature (morphology, surface characteristics, and optical properties) of the photocatalyst, role of co-catalyst/sacrificial reagents, mechanism, kinetics, etc. Nevertheless, there is still not many comprehensive studies to identify an appropriate sacrificial reagent with respect to the nature of a photocatalyst.

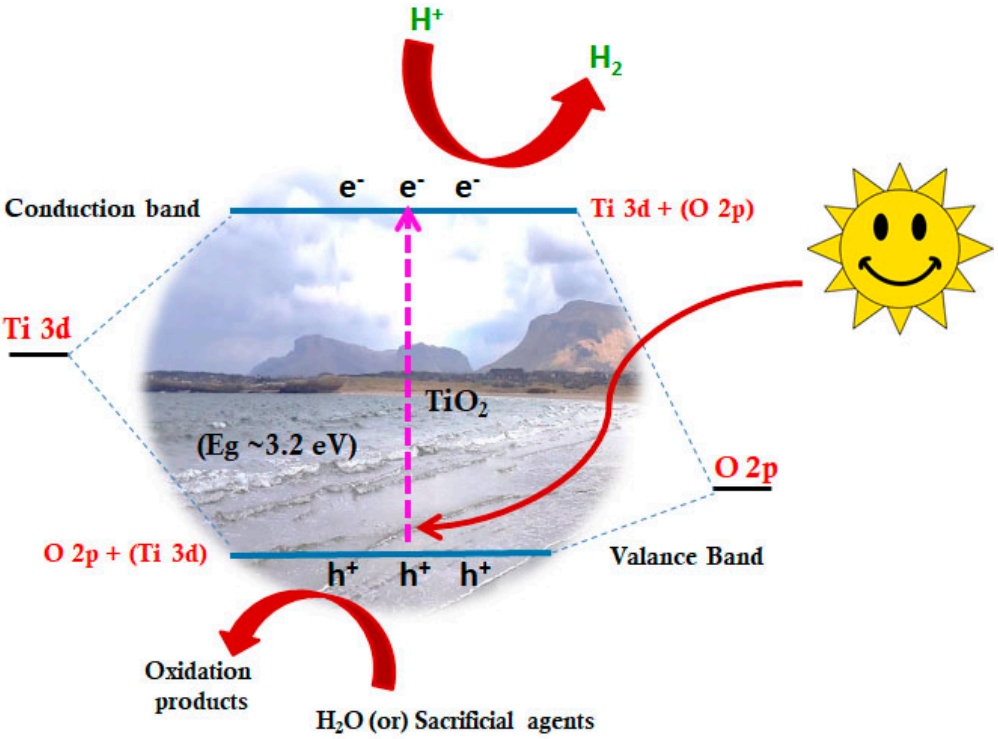

Figure 1. Schematic representation of the water-splitting process on a photocatalyst surface under light irradiation [1]. Reproduced with permission from Ref. [1]. Copyright 2019, Elsevier.

Sacrificial agents or electron donors/hole scavengers play a prominent role in photocatalytic H_2 production because the water splitting is energetically an uphill reaction (ΔH_0 = 286 kJ mol^{-1}). It is realized that methanol, triethanolamine, and sodium sulfide/sodium sulfite are the most commonly used sacrificial reagents for oxide, carbon, and sulfide photocatalysts, respectively. In most of the cases, fresh water (e.g., deionized water or double distilled water) has been used to evaluate the H_2 production efficiency in a micro photo-reactor (volume in the range of 30 to 70 mL) with a strong light irradiation source (nearly $\leq$ 300 W). However, the vitality and utilization of this technology have not been comprehensively studied in a real environment. Moreover, the commercialization of this technology is still restrained by its poor efficiency and the use of expensive noble metals (like Pt, Au, Pd, Rh) as co-catalysts. Most of the published results do not have much consistency in terms of efficiency. For example, different efficiency values have been reported for pure TiO_2 using methanol as a scavenger (Table 1). This discrepancy is ascribed to the following reasons: photo-reactor design, inert gas (Ar or N_2) purging flow rate, light irradiation source, gas sampling method, gas chromatography (GC) analysis conditions, calculations, etc.

Table 1. Photocatalytic H_2 production efficiency of TiO_2 using methanol sacrificial agent.

Catalyst Amount (g/L)	Concentration of Methanol (%)	Light Source	H_2 Production Efficiency (μmol/g/h)	Reference
1	10	300 W of Xe (without UV cutoff filter)	42.00	[420]
0.6	16.66	300 W of Xe (with UV cutoff filter)	18.47	[217]
0.5	20	300 W of Xe (with UV cutoff filter)	~20.00	[194]
1.29	25.8	300 W of Xe (with UV cutoff filter)	~2.00	[421]

The photochemical reactions of sacrificial agents (methanol, ethanol, isopropanol, ethylene glycol, glycerol, glucose, lactic acid, triethanolamine, sodium sulfide, sodium sulfite, and sodium sulfide/sodium sulfite mixture) and their degradation products during H_2 production are summarized as follows:

Methanol [422] (MeOH):

$$H_2O_{(l)} + h^+ \rightarrow {}^{\bullet}OH + H^+ \quad (1)$$

$$CH_3OH_{(l)} + {}^{\bullet}OH \rightarrow {}^{\bullet}CH_2OH + H_2O_{(l)} \quad (2)$$

$${}^{\bullet}CH_2OH \rightarrow HCHO_{(l)} + H^+ + e^- \quad (3)$$

$$2H^+ + 2e^- \rightarrow H_{2\,(g)} \quad (4)$$

$$HCHO_{(l)} + H_2O_{(l)} \rightarrow HCOOH_{(l)} + H_{2\,(g)} \quad (5)$$

$$HCOOH_{(l)} \rightarrow CO_{2\,(g)} + H_{2\,(g)} \quad (6)$$

Overall reaction:

$$CH_3OH_{(l)} + H_2O_{(l)} \rightarrow CO_{2\,(g)} + 3H_{2\,(g)} \quad (7)$$

Ethanol [423] (EtOH):

$$CH_3CH_2OH + TiO_2 \rightarrow {}_{(S)}\,CH_3CH_2O - Ti^{4+} + {}_{(S)}\,OH \quad (8)$$

$$TiO_2 + \text{UV light} \rightarrow 2e^-_{(a)} + 2h^+ \quad (9)$$

$${}_{(s)}\,CH_3CH_2O - Ti^{4+} + 2h^+ \rightarrow {}_{(S)}\,CH_3CHO + Ti^{4+} \quad (10)$$

$${}_{(s)}\,2OH + e^-_{(a)} \rightarrow H_2 + {}_{(S)}\,2O^{2+} \quad (11)$$

Here, (s) represents the photocatalyst surface and (a) denotes the photo-excited electrons by UV light.

Isopropanol [424] (IPA):

$$\left[{}^{S^2}_{Cd^{2+}} > (CdS)\right]_2 + H_2O \rightarrow {}^{S^2}_{Cd^{2+}} > Cd(II)SH + {}^{S^2}_{Cd^{2+}} > S(-II)Cd(II)OH \quad (12)$$

$${}^{S^{2-}}_{Cd^{2+}} > CdSH_2^+ \rightarrow {}^{S^{2-}}_{Cd^{2+}} > CdSH + H^+ \quad (13)$$

$${}^{S^{2-}}_{Cd^{2+}} > CdSH \rightarrow {}^{S^{2-}}_{Cd^{2+}} > CdS - + H^+ \quad (14)$$

$${}^{S^{2-}}_{Cd^{2+}} > CdOH_2^+ \rightarrow {}^{S^{2-}}_{Cd^{2+}} > CdOH + H^+ \quad (15)$$

$${}^{S^{2-}}_{Cd^{2+}} > CdOH \rightarrow {}^{S^{2-}}_{Cd^{2+}} > CdO - + H^+ \quad (16)$$

$$^{S^2}_{Cd^{2+}} > Cd(+II)S(0)^+ + C_3H_7OH \rightarrow ^{S^2}_{Cd^{2+}} > Cd(+II)S(-I)H^+ + C_3H_6^{\bullet}OH \quad (17)$$

$$^{S^{2-}}_{Cd^{2+}} > Cd(+II)S(-I)H^+ + C_3H_7OH \rightarrow ^{S^{2-}}_{Cd^{2+}} > Cd(+II)S(-II)H_2^+ + C_3H_6^{\bullet}OH \quad (18)$$

$$2H^{\bullet} \rightarrow H_2 \quad (19)$$

$$2\,C_3H_6^{\bullet}OH \rightarrow 2\,C_3H_5O + H_2 \quad (20)$$

$$^{S^2}_{Cd^{2+}} > Cd(+II)S(-II)H_2^+ \rightarrow ^{S^2}_{Cd^{2+}} > Cd(+II)S(-II)H + H^+ \quad (21)$$

$$^{S^{2-}}_{Cd^{2+}} > CdOH + e^-_{CB} \rightarrow ^{S^{2-}}_{Cd^{2+}} > CdO^- + H^+ \quad (22)$$

Ethylene Glycol [76,425] (EG):

$$OHCH_2 - CH_2OH + H_2O \xrightarrow{TiO_2,\ hv} OHCH_2 - CHO \quad (23)$$

$$OHCH_2 - CHO \xrightarrow{{}^{\bullet}OH} OHCH_2 - COOH \quad (24)$$

$$OHCH_2 - COOH \rightarrow CH_3COOH \quad (25)$$

$$OHCH_2 - COOH \rightarrow HOOC - COOH \quad (26)$$

$$HOOC - COOH \rightarrow HCOOH \quad (27)$$

$$HCOOH\ (or)\ CH_3COOH\ (or)\ HOOC - COOH \rightarrow CO_2 + H_2 + CH_4 + C_2H_4 + C_2H_6 + H_2O \quad (28)$$

Glycerol [130] (GLY):

$$C_3H_8O_3 + 3H_2O + 14\,h^+_{(VB)} \rightarrow \text{intermediates } (C_2H_4O_2,\ C_2H_2O_3,\ C_2H_4O_3,\ C_3H_6O_3,\ \text{etc}) \rightarrow 3CO_2 + 14\,H^+ \quad (29)$$

$$14H^+ + 14e^-_{CB} \rightarrow 7H_2\ (g) \quad (30)$$

Glucose [9] (GLU):

$$C_6H_{12}O_6 + H_2O\ (\text{anaerobic}) \rightarrow C_5H_{10}O_5 + HCOOH + H_{2(g)} \quad (31)$$

$$C_5H_{10}O_5 + H_2O \rightarrow C_4H_8O_4 + HCOOH + H_{2\ (g)} \quad (32)$$

$$C_4H_8O_4 + H_2O + HCOOH + H_{2\ (g)}(\text{aerobic}) \rightarrow HCOOH + H_{2(g)} + CO_{2\ (g)} \quad (33)$$

$$C_6H_{12}O_6 \xrightarrow{TiO_2,\ hv,H_2O,\ O_2} C_6H_{12}O_7 \quad (34)$$

$$C_6H_{12}O_7 \xrightarrow{TiO_2,\ hv,H_2O,\ O_2} C_6H_{10}O_8 \quad (35)$$

$$C_6H_{10}O_8 \xrightarrow{TiO_2,\ hv,H_2O,\ O_2} HCOOH + H_{2(g)} + CO_{2(g)} \quad (36)$$

Lactic Acid [426] (LA):

$$CH_3 - CH(OH) - COOH + H_2O \xrightarrow{TiO_2,\ hv} CO_2 + H_2 + CH_3 - CO - COOH \quad (37)$$

Triethanolamine [427] (TEOA):

$$C_6H_{15}NO_3 \rightarrow C_6H_{15}NO_3^+ + e^- \quad (38)$$

$$C_6H_{15}NO_3^+ \rightarrow C_6H_{14}NO_3^{\bullet} + H^+ \quad (39)$$

$$C_6H_{14}NO_3^{\bullet} \rightarrow C_6H_{14}NO_3^+ + e^- \quad (40)$$

$$C_6H_{14}NO_3^+ + H_2O \rightarrow C_4H_{11}NO_3 + CH_3CHO + H^+ \quad (41)$$

Sodium sulfide (Na_2S) [428]:

$$Na_2S + H_2O \rightarrow 2Na^+ + S^{2-} \quad (42)$$

$$S^{2-} + H_2O \rightarrow HS^- + OH^- \quad (43)$$

$$HS^- + hv \rightarrow HS^{-*} \quad (44)$$

$$HS^{-*} + HS^- \rightarrow [(HS)_2]^{-*} \rightarrow H_2 + S_2^{2-} \quad (45)$$

Sodium sulfite (Na_2SO_3) [429]:

$$\text{Irradiation}: SO_3^{2-} \xrightarrow{hv} SO_3^{2-*} \quad (46)$$

$$\text{Oxidation}: SO_3^{2-*} + 2OH^- \rightarrow SO_4^{2-} + H_2O + 2e^- \quad (47)$$

$$\text{Reduction}: 2H_2O + 2e^- \rightarrow H_2 + 2OH^- \quad (48)$$

$$\text{Oxidation}: 2SO_3^{2-} \rightarrow S_2O_6^{2-} + 2e^- \quad (49)$$

$$\text{Reduction}: 2H_2O + 2e^- \rightarrow H_2 + 2OH^- \quad (50)$$

Sodium sulfide and sodium sulfite mixture (Na_2S and Na_2SO_3) [430]:

Two different reaction pathways are involved when sodium sulfide and sodium sulfite mixture is used as a sacrificial agent.

$$HS^-_{(aq)} \rightarrow HS^-_{(ads)} \quad (51)$$

$$HS^-(ads) \xrightarrow{hv} [HS^-(ads)]^* \quad (52)$$

Path A:

$$[HS^-(ads)]^* \rightarrow H^* + S^-(ads) \quad (53)$$

$$S^-(ads) + [HS^-(ads)]^* \rightarrow \left[HS_2^{2-}\right]\varphi \quad (54)$$

$$\left[HS_2^{2-}\right]\varphi \rightarrow H^* + S_2^{2-}(ads) \quad (55)$$

$$2H^* \rightarrow H_2 \quad (56)$$

Path B:

$$\left[HS^-(ads)\right]^* + S^0(ads) \rightarrow [HS_2^-]\varphi \quad (57)$$

$$[HS_2^-]\varphi + OH^- + SO_3^{2-} + S^0(ads) \rightarrow \left[HS_2^{2-}\right]\varphi + OH^\bullet + S_2O_3^{2-} \quad (58)$$

$$OH^\bullet + SO_3^{2-} \xrightarrow{hv} SO_4^{2-} + H^* \quad (59)$$

$$2H^* \rightarrow H_2 \quad (60)$$

$$[HS^-(ads)]^* + H_2O \rightarrow S^0(ads) + H_2 + OH^- \quad (61)$$

$$\left[HS_2^-\right]\varphi + OH^- \rightarrow H_2O + S_2^{2-} \quad (62)$$

where (ads) denotes adsorption and φ represents species, which can undergo intramolecular charge transfer.

The previous articles reported H_2 production efficiencies with various combinations of photocatalysts and sacrificial reagents. This study provides detailed information on the selection of sacrificial reagents and photocatalysts for H_2 production. The efficiencies of TiO_2-P25, *g*-C_3N_4, and CdS were evaluated using methanol (MeOH), ethanol (EtOH), isopropanol (IPA), ethylene glycol

(EG), glycerol (GLY), lactic acid (LA), glucose (GLU), sodium sulfide (Na_2S), sodium sulfite (Na_2SO_3), sodium sulfide/sodium sulfite mixture (Na_2S/Na_2SO_3), and triethanolamine (TEOA) as sacrificial reagents (organic and inorganic). The efficiency of a photocatalyst was described in terms of pH of medium and nature of the sacrificial agent (carbon chain length, alpha hydrogen, hydroxyl groups, binding interactions, etc). Besides, control experiments were executed to investigate the H_2 production with only sacrificial reagents under solar light irradiation in the absence of photocatalyst.

2. Results and Discussion

2.1. TiO_2 P25

Figure 2 shows the H_2 production efficiency of TiO_2 P25 using various sacrificial agents. H_2 production efficiencies of TiO_2/EG, TiO_2/GLY, $TiO_2/Na_2S/Na_2SO_3$, TiO_2/GLU, TiO_2/Na_2S were found to be 190.2 µmol, 130.8 µmol, 126 µmol, 120 µmol, and 120 µmol, respectively. H_2 production efficiency of TiO_2/MeOH system reduced to 81.6 µmol for the same period. The use of TEOA, EtOH, IPA, and Na_2SO_3 as sacrificial reagents resulted in poor H_2 production, yielding 61.8 µmol, 49.8 µmol, 46.2 µmol, and 40.8 µmol, respectively. TiO_2/LA mixture displayed the lowest yield of H_2 production (only 27.6 µmol). TiO_2/EG mixture showed the maximum H_2 production (190.2 µmol) efficiency as compared to all other combinations. This is ascribed to the faster charge transfer reaction in the TiO_2/EG system compared to the photo-generated electron-hole recombination process [431,432]. The length of the carbon chain, the number of hydroxyl groups, and dehydrogenation/decarbonylation characteristics of sacrificial agents are the primary features in controlling the H_2 production efficiency. Moreover, the following properties of sacrificial agents could also strongly influence the efficiency: polarity and electron donating ability, adsorption capability on the photocatalyst surface, the formation of by-products, and the selectivity for reaction with photo-generated holes (e.g., decarboxylation process) [10,94,431–436]. Carbon monoxide (CO) is one of the main intermediates for the alcohols with a short carbon chain. Hence, the adsorption of CO on the active sites of TiO_2 via chemisorption restricts further adsorption of alcohol on the photocatalyst surface [437]. The removal of CO as CO_2 is the rate-determining step in H_2 production. It depends on the adsorption efficiency and the number of alpha hydrogens of the sacrificial agent [437]. During the water-splitting process, the hydroxyl radical ($^{\bullet}OH$) abstracts alpha hydrogen from the alcohol to create $^{\bullet}RCH_2$-OH radical, which gets further oxidized into an aldehyde, carboxylic acid, and CO_2 [437]. Bahruji et al. [437] suggested that alkyl groups connected to the alcohol (e.g., C_xH_yOH) could yield the respective alkanes (e.g., C_{x-1}) during the water-splitting process. The alkane production rate was decreased with the increase of OH groups in alcohol [438]. In the case of polyols, the hydrogen atoms from the alpha carbon could be easily extracted and evolved in the form of H_2 [438]. The alpha carbon atoms could be oxidized into CO_2. The C atoms without OH groups (other than alpha C atoms) would be evolved in the form of alkanes [438]. Time-resolved transient absorption spectroscopy results revealed that carbohydrates and polyols (C2–C6) could rapidly react with ~50–60% holes (h^+) within 6 ns as compared to other alcohols [439,440]. The OH groups could act as an anchor for the chemisorption of alcohols on the photocatalyst surface [438]. The coordination efficiency of alcohols with the Ti sites relies on the number of OH groups and the carbon chain length. This type of linkage could be beneficial for the utilization of holes to improve the H_2 production and suppress the charge carrier recombination [438]. The first principle calculations showed that the formation of gap levels in TiO_2 via the adsorption polyols could accelerate the hole trapping process [441]. Though EG showed maximum efficiency for TiO_2-P25, glycerol and glucose are the most appropriate sacrificial agents for any kind of oxide photocatalyst. This owes to their (glucose and glycol) most abundance, less toxicity, low cost, and they can readily undergo dehydrogenation as compared to other alcohols [40,63,435].

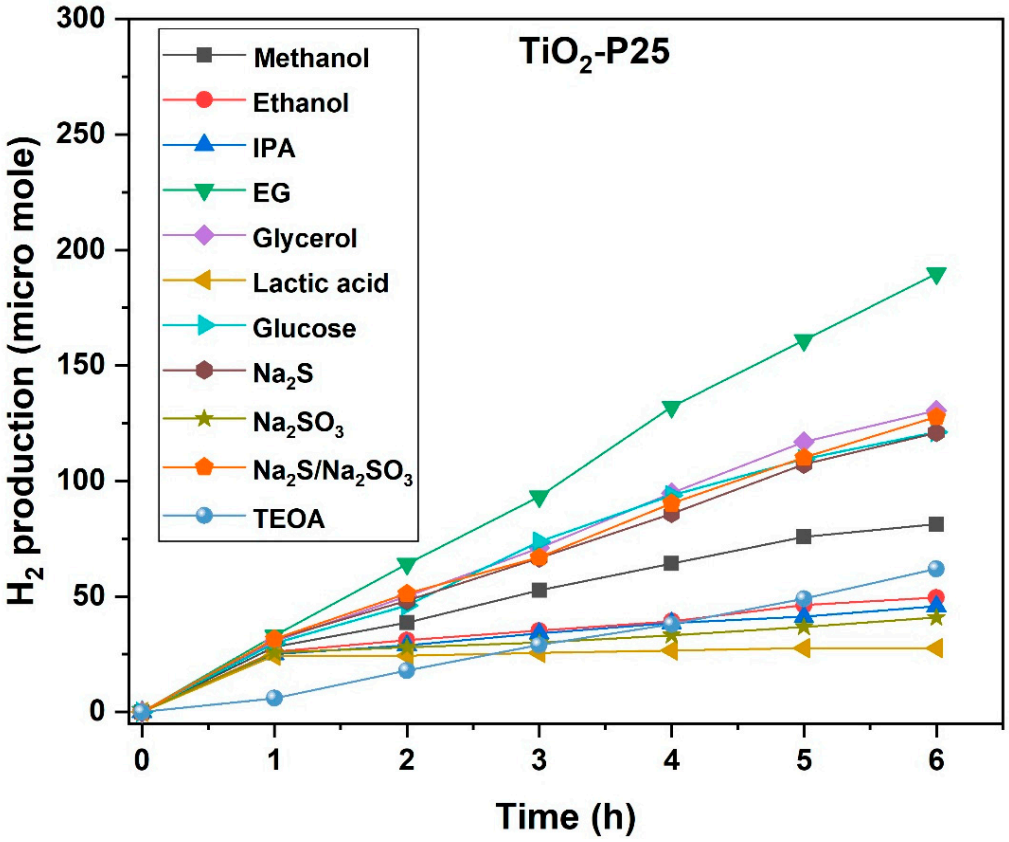

Figure 2. Photocatalytic H_2 production efficiency of TiO_2-p25 using various sacrificial agents.

2.2. *g*-C_3N_4

H_2 production efficiency of *g*-C_3N_4 with various sacrificial agents is shown in Figure 3. In this case, only the use of TEOA, Na_2S, Na_2SO_3, and Na_2S/Na_2SO_3 resulted in H_2 production. H_2 production efficiency of *g*-C_3N_4/Na_2S (139.8 µmol) system was higher than that of *g*-C_3N_4/Na_2S/Na_2SO_3 (127.2 µmol) and *g*-C_3N_4/Na_2SO_3 (5.4 µmol). *g*-C_3N_4/TEOA mixture showed the best efficiency (247.2 µmol) when compared to all other sacrificial agents. This can be ascribed to the fact that photo-corrosion and degradation of π conjugated structure [304] of amine rich *g*-C_3N_4 is secured by the effective binding of TEOA on the catalyst surface [112]. TEOA excellently consumes the photo-generated holes, improves the dispersion of photocatalyst, and acts as a binding ligand to improve the interaction of *g*-C_3N_4 with water molecules [204,442]. The results shown in Figure 3 also suggest that alcohols and glucose are not strongly adsorbed on the *g*-C_3N_4 surface for water-splitting reaction. This is attributed to the absence of hydrophilicity and surface characteristics (e.g., active sites, poor electrical conductivity, water oxidation ability) of *g*-C_3N_4 to facilitate a strong interfacial electron/hole transfer process on the catalyst surface. The poor crystallinity and basal planar structure of *g*-C_3N_4 endorse the electron-hole recombination [443]. Moreover, high activation energy and overpotential are required for H_2 production on the *g*-C_3N_4 surface [182,211]. This could be rectified by the loading of noble metals or co-catalysts over *g*-C_3N_4 or fabricating Z-scheme photocatalysts. In most of the studies, it was reported that *g*-C_3N_4 acts as an outstanding template and there was no H_2 production on *g*-C_3N_4 without any noble metal co-catalyst [444,445]. The results also demonstrated that the light absorption capability, chemical stability, and suitable band edge positions of narrow band-gap *g*-C_3N_4 are not the only decisive factors to enhance the H_2 production efficiency.

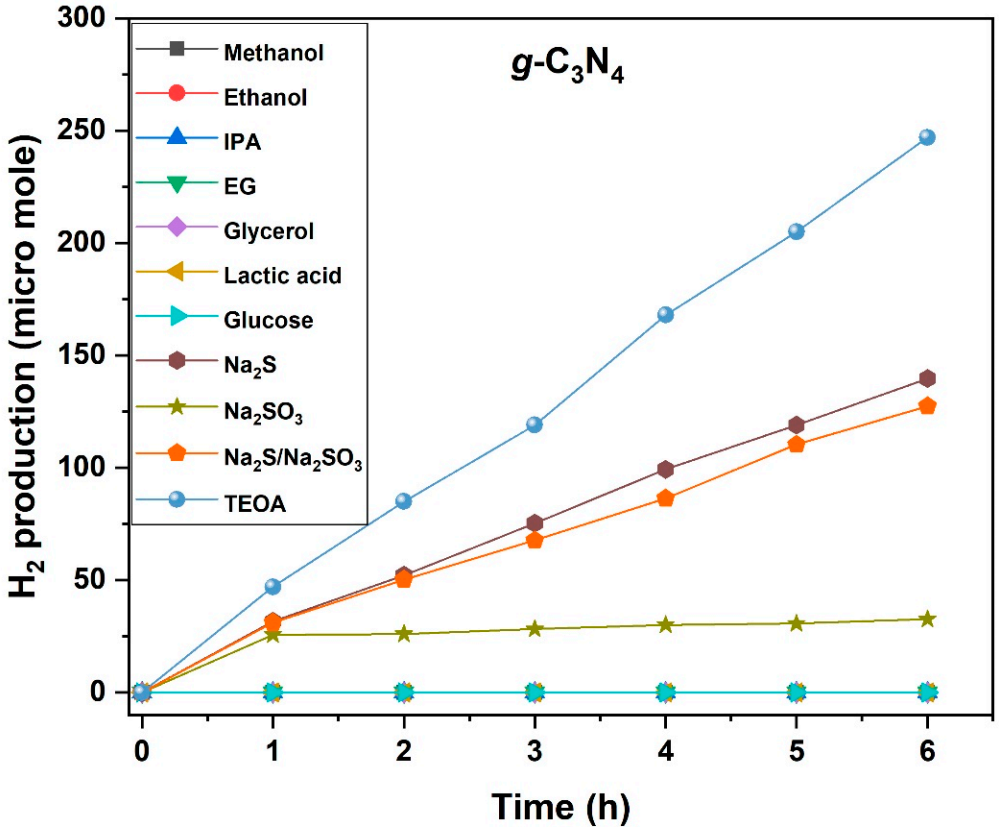

Figure 3. Photocatalytic H_2 production efficiency of *g*-C_3N_4 using various sacrificial agents.

2.3. CdS

Photocatalytic H_2 production efficiency of CdS using various sacrificial agents is shown in Figure 4. The use of TEOA, Na_2S, Na_2SO_3, Na_2S/Na_2SO_3, and LA as sacrificial reagents resulted in H_2 formation. CdS/TEOA system showed the maximum efficiency of 283.2 µmol of H_2 as compared to all other sacrificial agents. The efficiency of CdS/Na_2S, CdS/Na_2SO_3, CdS/LA systems was found to be 181.2 µmol, 154.8 µmol, and 84 µmol, respectively. The mixture of CdS/Na_2S/Na_2SO_3 showed the lowest H_2 production of 54 µmol after 6 h. Bare CdS is not stable under prolonged light irradiation because the sulfide ions on its surface are rapidly oxidized into sulfur through the reaction with photo-generated holes (photo-corrosion – $CdS + 2h^+ \rightarrow Cd^{2+} + S$) [308,446,447]. The sulfide oxidation of CdS can occur before the oxidation of water by holes [308,447]. Hence, the H_2 production efficiency of CdS highly relies on the effective binding of sacrificial agents on its surface. The results showed that amine and sulfide/sulfite might be strongly bound to the CdS surface and it could effectively consume the holes as compared to alcohol and sugars. It is obviously noted that H_2 is produced in high alkaline (amine, sulfide, and sulfite) and acidic (LA) pH mixtures when compared to neutral pH (alcohols and sugar). LA is converted into pyruvic acid and CO_2 during the water-splitting reaction; this may slightly influence the pH and polarity of the reaction mixture. The sulfide ions from Na_2S stabilizes CdS surface to terminate the surface defects originated from photo-corrosion. The electron-hole recombination process is strongly restrained by the sulfide ions at alkaline pH. When CdS is suspended in a water medium, thiol (Cd-SH) and hydroxyl (Cd-OH) groups are developed on its surface, which are highly pH dependent [310]. In the case of Na_2S, the pH of the medium is alkaline, sulfide (S_2^-) and hydrogen sulfide (HS^-) are formed when Na_2S is dissolved in water [310]. During light irradiation, S_2^- and HS^- are quickly oxidized into sulfate (SO_4^{2-}) and polysulfide (S_4^{2-}, S_5^{2-}) ions, respectively [310]. The oxidation of sulfide by the photo-generated holes is much preferential as compared to the photo-corrosion of CdS [112]. The precipitation of yellow colored polysulfide ions diminishes the photocatalytic efficiency via acting as an optical filter and competing

with the H_2 generation reaction. This could be restricted by the addition of Na_2SO_3 to generate more HS^- and $S_2O_3^{2-}$ ions to enhance the photocatalytic activity [292]. However, the results shown in Figure 4 suggest that H_2 production efficiency of Na_2S/CdS or CdS/Na_2SO_3 are higher than that of CdS/Na_2S/Na_2SO_3. The reasons could be predicted by the photolysis experiments of sacrificial agents. The pH of TEOA/water mixture would be around 12, which could enhance the H_2 production efficiency via strong interfacial bonding on the CdS surface and its reaction with photo-generated holes [204].

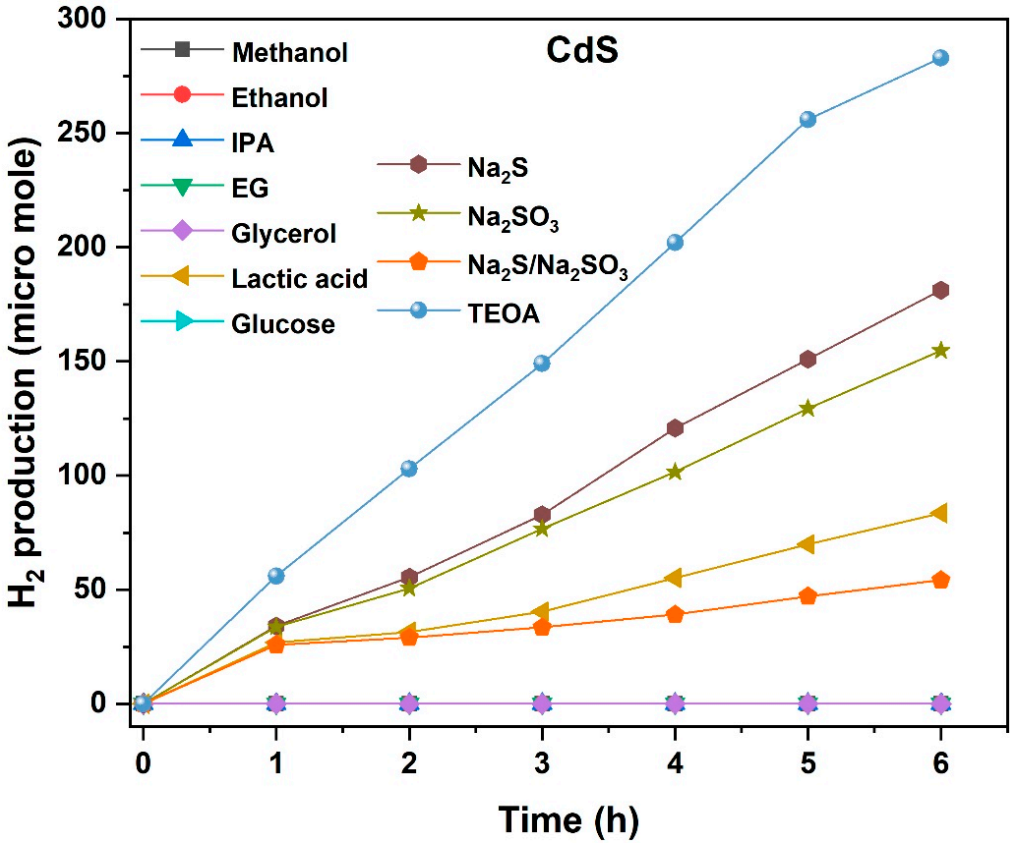

Figure 4. Photocatalytic H_2 production efficiency of CdS using various sacrificial agents.

2.4. Photolysis

Photolysis experiments were carried out for all sacrificial agents in water for 6 h of light irradiation without the additions of photocatalysts. Control experiments were also carried out in the absence of sacrificial agents to evaluate the efficiency of the photocatalyst. There was no H_2 production in the absence of any sacrificial agents for TiO_2-p25, *g*-C_3N_4, and CdS. The results of photolysis experiments with sacrificial reagents under solar light in the absence of photocatalysts are shown in Figure 5. Interestingly, a remarkable amount of H_2 was evolved from Na_2S/water (159 µmol), Na_2SO_3/water (51 µmol), and Na_2S/Na_2SO_3/water (134.4 µmol) systems without photocatalyst. It was observed that the H_2 production efficiency was increased with respect to the concentration of sulfide or sulfite. When compared to results obtained in the presence of photocatalysts, it could be observed that the photocatalysts, such as TiO_2-p25 and *g*-C_3N_4, surprisingly reduced the actual H_2 production efficiency of sulfide system. There was not a significant increment in the efficiency of CdS/Na_2S as compared to the photolysis of Na_2S. However, the efficiency of CdS/Na_2SO_3 was higher than that of Na_2SO_3 photolysis. It is also noted that a high concentration of sulfide/sulfite mixture (in the range of 0.2 M to 1 M) was used in most of the studies for H_2 production [246,264,273,300,448–451]. In such cases, the photolysis of sulfide or sulfite solutions were not evaluated. Hence, the H_2 production should have been mainly originated via photolysis of sulfide/sulfite mixture rather than the photocatalytic

effect. The photochemical reactions involved in H_2 generation from sulfide and sulfite solutions are described in detail from Equations (42)–(62) [428–430].

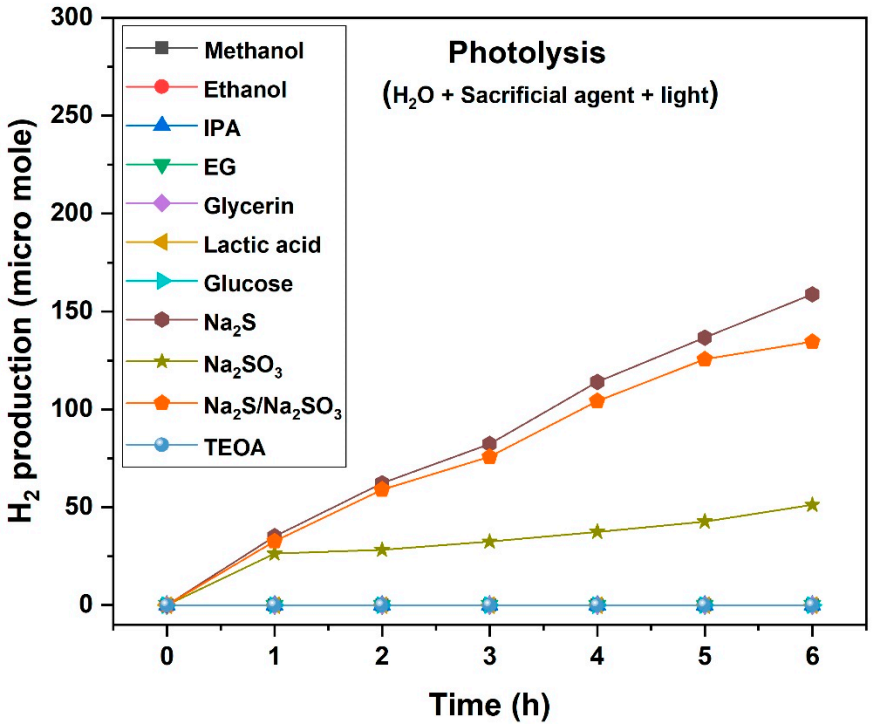

Figure 5. H_2 production efficiency of sacrificial agents without photocatalyst (photolysis).

Li et al. [430] investigated the photochemical generation of H_2 from sulfide and sulfite mixture solutions. They found that the pH of sulfide/sulfite mixture (~13.14) was slightly decreased (~12.94) after the completion of photolysis experiments. The addition of a small amount of sulfite into the sulfide solution could not amplify the H_2 production. Nevertheless, the elemental sulfur or polysulfide originated from HS^- is efficiently consumed by SO_3^{2-} to improve the photonic efficiency. It is strongly recommended to study the effect of photolysis when the sulfide/sulfite mixture is used as the sacrificial agent to evaluate the H_2 production efficiency of the photocatalyst. The elemental sulfur could be filtered out by passing hydrogen sulfide (H_2S) gas in the aqueous solution under nitrogen atmosphere [428]. The resulting filtrate could be reused for photolytic H_2 production [428].

Wang et al. [112] suggested that Na_2S/Na_2SO_3, MeOH, and TEOA were the most appropriate sacrificial agents for sulfide, oxide, and carbon-based photocatalysts. However, the experiments were not performed to study the effect of photolysis, especially the sulfide or sulfite solutions. A high concentration of sacrificial agents was used to evaluate the photocatalytic activity. The photocatalytic experiments were not described in detail. Moreover, the effect of most earth abundant glucose and glycerol were not investigated on the H_2 production efficiency. Sulfur dioxide (SO_2) emission from the flue gas can be absorbed as Na_2SO_3 solution using dilute sodium hydroxide. The photolysis of such sodium sulfite solution is an eco-friendly way to produce H_2 gas [429]. Only a few studies were focused on using wastewater for H_2 generation. Souza and Silva [310] studied the feasibility of using tannery sludge wastewater for photocatalytic H_2 generation using CdS. The photolysis of sulfide-rich wastewater or industrial effluent is the foremost choice to produce green energy in a sustainable way via photocatalysis.

2.5. TOC Analysis

TOC analysis was carried out for solutions after the photocatalytic experiments, to assess the degradation of organic sacrificial agents in the solutions at the end of 6 h experiment. Table 2

summarizes the TOC results for the solutions of TiO_2-p25. The results suggest the effective utilization of the organic sacrificial agents by TiO_2-P25 for H_2 production. TOC was reduced almost half for most of the sacrificial agents after 6 h except for glucose. This is ascribed to the formation of more organic intermediates when glucose is utilized as the sacrificial agent.

Table 2. TOC of solutions after the completion of the photocatalytic reaction.

Sample	TOC (mg/L)	
	Blank (Before Light Irradiation)	TiO_2-P25
Water	8.659	-
Methanol	30,450	15,530
Ethanol	43,680	17,070
Isopropanol	55,010	17,770
Glycerol	54,220	18,700
Ethylene glycol	59,080	17,930
Glucose	7699	11,500
Lactic acid	47,310	20,440

3. Experimental

All the chemicals used were of analytical grade and used as received without further purification. TiO_2 P25 was purchased from Sigma Aldrich (Darmstadt, Germany), *g*-C_3N_4 was synthesized by the calcination of urea at 550 °C for 2 h [452]. CdS was synthesized via the hydrothermal method [453]. Photocatalytic experiments were carried out using an immersion type reactor (Lelesil innovative systems, Thane, Maharashtra, India) as shown in Figure 6. All the reactions were carried out without any noble metal co-catalyst. The reactor is a tightly closed setup with a total volume of 1000 mL. Reactions were carried out using 500 mL of double distilled water with 0.5 g/L of photocatalyst and desired amount of sacrificial reagent (based on the literature). The empty headspace was kept constant at 500 mL for all reactions. The sacrificial agent concentration was fixed at 10% (alcohol, amine, acid) and 0.1 M (glucose, sodium sulfide, sodium sulfite, sodium sulfide/sodium sulfite mixture). The mixture was stirred under nitrogen purging for 1 h after which, the purging was stopped, and the reactor was closed immediately. The mixture was irradiated using a 300 W Xenon arc lamp without any UV cutoff filter (simulated solar light source). H_2 sampling was carried out for every 1 h using a 250 µL sample lock gas tight syringe. At the end of the photoreaction time, when organic sacrificial reagents were used, the mixture was filtered using a 0.45 µm micro-filter, and the filtrate was analyzed using a total organic carbon (TOC; Shimadzu, Japan) analyzer to measure the loss of reagents by mineralization. H_2 was analyzed using Agilent gas chromatography (USA) with thermal conductivity detector (TCD), manual injection, carrier gas N_2, molecular sieve 5 A° column with 2-m length, front inlet temperature 140 °C, and detector temperature 150 °C.

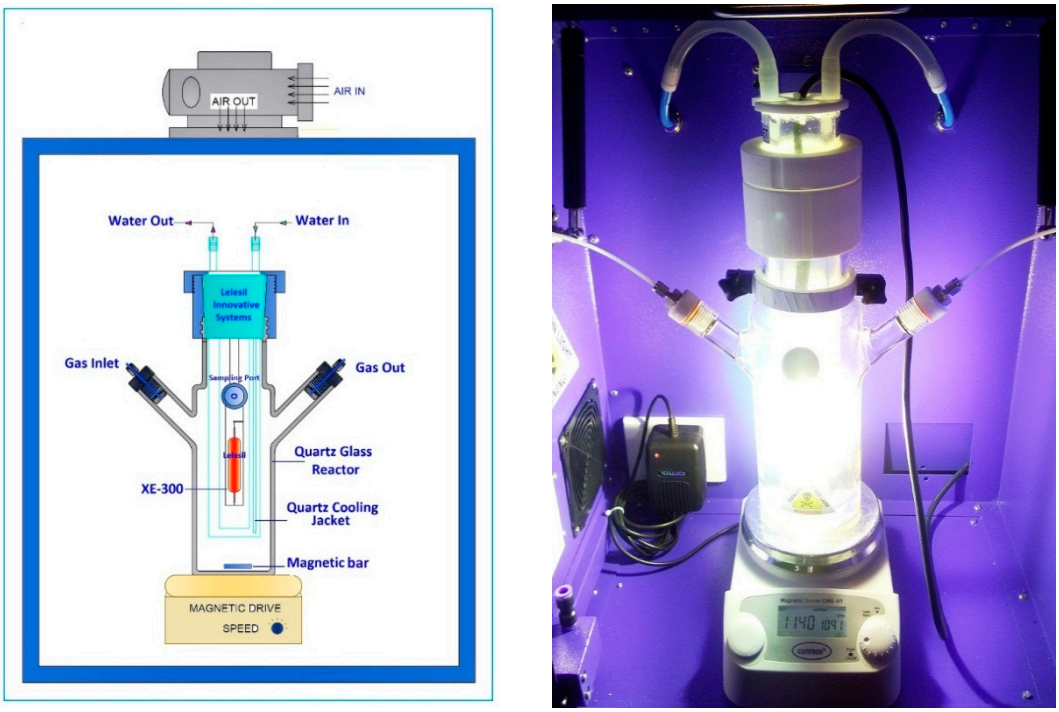

(**a**) (**b**)

Figure 6. (**a**) Schematic and (**b**) photograph of the reactor used for photocatalytic H_2 production.

4. Summary and Outlook

Different types of photocatalysts have been successfully investigated for H_2 production using various organic and inorganic sacrificial agents. The surface of an oxide photocatalyst would be more suitable for polyols and sugars for adsorption as compared to amines and sulfides. Amines are the most appropriate of sacrificial agents for carbon and sulfide photocatalysts. CdS/TEOA (283.2 µmol), *g*-C_3N_4/TEOA (247.2 µmol), and TiO_2/EG (190.2 µmol) are the three best systems with maximum H_2 production in this study. H_2 could also be generated via the direct photolysis of sodium sulfide solution in the absence of any catalyst. TiO_2-p25 and *g*-C_3N_4 suppress the self-H_2 generation efficiency of Na_2S photolysis. More technological developments are required for the practical application of water-splitting in a scalable and economically feasible way. Stable, affordable, and active co-catalysts should be developed in the future to replace the expensive noble metals to achieve a significant amount of H_2 production. In most of the studies, precious fresh water with a high concentration of sacrificial agents was used in a small reactor to generate H_2. Hence, future studies should be focused on a pilot scale using industrial wastewater and seawater rather than using fresh water.

Author Contributions: Conceptualization V.K. and A.A-W.; Supervision, V.K., A.A-W. and M.K.; Methodology, design, investigation, data creation and analysis, V.K.; Methodology, data analysis, and original draft preparation, M.D.I and A.B.; Methodology and data analysis, J.Y.D. and R.K.C.

Funding: The authors are grateful to Texas A&M University at Qatar and Qatar Foundation for financial support.

Conflicts of Interest: The authors declare no conflict of interest.

References

1. Kumaravel, V.; Mathew, S.; Bartlett, J.; Pillai, S.C. Photocatalytic hydrogen production using metal doped TiO_2: A review of recent advances. *Appl. Catal. B Environ.* **2019**, *244*, 1021–1064. [CrossRef]
2. Fujishima, A.; Honda, K.J. Electrochemical photolysis of water at a semiconductor electrode. *Nature* **1972**, *238*, 37–38. [CrossRef] [PubMed]

3. Abdullah, H.; Kuo, D.-H.; Chen, X. High efficient noble metal free Zn (O, S) nanoparticles for hydrogen evolution. *Int. J. Hydrogen Energy* **2017**, *42*, 5638–5648. [CrossRef]
4. Agegnehu, A.K.; Pan, C.-J.; Tsai, M.-C.; Rick, J.; Su, W.-N.; Lee, J.-F.; Hwang, B.-J. Visible light responsive noble metal-free nanocomposite of V-doped TiO_2 nanorod with highly reduced graphene oxide for enhanced solar H_2 production. *Int. J. Hydrogen Energy* **2016**, *41*, 6752–6762. [CrossRef]
5. Alharbi, A.; Alarifi, I.M.; Khan, W.S.; Asmatulu, R. Synthesis and analysis of electrospun $SrTiO_3$ nanofibers with NiO nanoparticles shells as photocatalysts for water splitting. In Proceedings of the 14th Brazilian Polymer Conference, São Paulo, Brazil, 22–26 October 2017; 22-26.
6. Al-Mayman, S.I.; Al-Johani, M.S.; Mohamed, M.M.; Al-Zeghayer, Y.S.; Ramay, S.M.; Al-Awadi, A.S.; Soliman, M.A. TiO_2 ZnO photocatalysts synthesized by sol–gel auto-ignition technique for hydrogen production. *Int. J. Hydrogen Energy* **2017**, *42*, 5016–5025. [CrossRef]
7. Bai, Y.; Chen, T.; Wang, P.; Wang, L.; Ye, L. Bismuth-rich $Bi_4O_5X_2$ (X = Br, and I) nanosheets with dominant {101} facets exposure for photocatalytic H_2 evolution. *Chem. Eng. J.* **2016**, *304*, 454–460. [CrossRef]
8. Barreca, D.; Carraro, G.; Gasparotto, A.; Maccato, C.; Warwick, M.E.; Toniato, E.; Gombac, V.; Sada, C.; Turner, S.; Van Tendeloo, G. Iron–Titanium Oxide Nanocomposites Functionalized with Gold Particles: From Design to Solar Hydrogen Production. *Adv. Mater. Interfaces* **2016**, *3*, 1600348. [CrossRef]
9. Bellardita, M.; García-López, E.I.; Marcì, G.; Palmisano, L. Photocatalytic formation of H_2 and value-added chemicals in aqueous glucose (Pt)-TiO_2 suspension. *Int. J. Hydrogen Energy* **2016**, *41*, 5934–5947. [CrossRef]
10. Beltram, A.; Romero-Ocana, I.; Jaen, J.J.D.; Montini, T.; Fornasiero, P. Photocatalytic valorization of ethanol and glycerol over TiO_2 polymorphs for sustainable hydrogen production. *Appl. Catal. A Gen.* **2016**, *518*, 167–175. [CrossRef]
11. Betzler, S.B.; Podjaski, F.; Beetz, M.; Handloser, K.; Wisnet, A.; Handloser, M.; Hartschuh, A.; Lotsch, B.V.; Scheu, C. Titanium Doping and Its Effect on the Morphology of Three-Dimensional Hierarchical Nb_3O_7 (OH) Nanostructures for Enhanced Light-Induced Water Splitting. *Chem. Mater* **2016**, *28*, 7666–7672. [CrossRef]
12. Cargnello, M.; Montini, T.; Smolin, S.Y.; Priebe, J.B.; Jaén, J.J.D.; Doan-Nguyen, V.V.; McKay, I.S.; Schwalbe, J.A.; Pohl, M.-M.; Gordon, T.R. Engineering titania nanostructure to tune and improve its photocatalytic activity. *Proc. Natl. Acad. Sci.* **2016**, *113*, 3966–3971. [CrossRef]
13. Cha, G.; Altomare, M.; Truong Nguyen, N.; Taccardi, N.; Lee, K.; Schmuki, P. Double-Side Co-Catalytic Activation of Anodic TiO_2 Nanotube Membranes with Sputter-Coated Pt for Photocatalytic H_2 Generation from Water/Methanol Mixtures. *Chem. Asian J.* **2017**, *12*, 314–323. [CrossRef]
14. Yuan, Q.; Liu, D.; Zhang, N.; Ye, W.; Ju, H.; Shi, L.; Long, R.; Zhu, J.; Xiong, Y. Noble-Metal-Free Janus-like Structures by Cation Exchange for Z-Scheme Photocatalytic Water Splitting under Broadband Light Irradiation. *Angew. Chem.* **2017**, *129*, 4270–4274. [CrossRef]
15. Chen, L.; Gu, Q.; Hou, L.; Zhang, C.; Lu, Y.; Wang, X.; Long, J. Molecular p–n heterojunction-enhanced visible-light hydrogen evolution over a N-doped TiO_2 photocatalyst. *Catal. Sci. Technol.* **2017**, *7*, 2039–2049. [CrossRef]
16. Chen, W.; Liu, H.; Li, X.; Liu, S.; Gao, L.; Mao, L.; Fan, Z.; Shangguan, W.; Fang, W.; Liu, Y. Polymerizable complex synthesis of $SrTiO_3$:(Cr/Ta) photocatalysts to improve photocatalytic water splitting activity under visible light. *Appl. Catal. B Environ.* **2016**, *192*, 145–151. [CrossRef]
17. Xiang, Q.; Cheng, F.; Lang, D. Hierarchical Layered WS_2/Graphene-Modified CdS Nanorods for Efficient Photocatalytic Hydrogen Evolution. *ChemSusChem* **2016**, *9*, 996–1002. [CrossRef] [PubMed]
18. Chen, Z.; Wu, Y.; Wang, Q.; Wang, Z.; He, L.; Lei, Y.; Wang, Z. Oxygen-rich carbon-nitrogen quantum dots as cocatalysts for enhanced photocatalytic H_2 production activity of TiO_2 nanofibers. *Prog. Nat. Sci. Mater. Int.* **2017**, *37*, 333–337. [CrossRef]
19. Clarizia, L.; Vitiello, G.; Luciani, G.; Di Somma, I.; Andreozzi, R.; Marotta, R. In situ photodeposited nanoCu on TiO_2 as a catalyst for hydrogen production under UV/visible radiation. *Appl. Catal. A Gen.* **2016**, *518*, 142–149. [CrossRef]
20. Dhanalaxmi, K.; Yadav, R.; Kundu, S.K.; Reddy, B.M.; Amoli, V.; Sinha, A.K.; Mondal, J. $MnFe_2O_4$ Nanocrystals Wrapped in a Porous Organic Polymer: A Designed Architecture for Water-Splitting Photocatalysis. *Chem. Eur. J.* **2016**, *22*, 15639–15644. [CrossRef] [PubMed]
21. Ding, J.; Ming, J.; Lu, D.; Wu, W.; Liu, M.; Zhao, X.; Li, C.; Yang, M.; Fang, P. Study of the enhanced visible-light-sensitive photocatalytic activity of Cr_2O_3-loaded titanate nanosheets for Cr (vi) degradation and H_2 generation. *Catal. Sci. Technol.* **2017**, *7*, 2283–2297. [CrossRef]

22. Elbanna, O.; Kim, S.; Fujitsuka, M.; Majima, T. TiO_2 mesocrystals composited with gold nanorods for highly efficient visible-NIR-photocatalytic hydrogen production. *Nano Energy* **2017**, *35*, 1–8. [CrossRef]
23. Escobedo, S.; Serrano, B.; Calzada, A.; Moreira, J.; de Lasa, H. Hydrogen production using a platinum modified TiO_2 photocatalyst and an organic scavenger. Kinetic modeling. *Fuel* **2016**, *181*, 438–449. [CrossRef]
24. Feng, N.; Liu, F.; Huang, M.; Zheng, A.; Wang, Q.; Chen, T.; Cao, G.; Xu, J.; Fan, J.; Deng, F. Unravelling the Efficient Photocatalytic Activity of Boron-induced Ti3+ Species in the Surface Layer of TiO_2. *Sci. Rep.* **2016**, *6*, 34765. [CrossRef] [PubMed]
25. Fiorenza, R.; Bellardita, M.; D'Urso, L.; Compagnini, G.; Palmisano, L.; Scirè, S. Au/TiO_2-CeO_2 Catalysts for Photocatalytic Water Splitting and VOCs Oxidation Reactions. *Catalysts* **2016**, *6*, 121. [CrossRef]
26. Fontelles-Carceller, O.; Muñoz-Batista, M.J.; Conesa, J.C.; Fernández-García, M.; Kubacka, A. UV and visible hydrogen photo-production using Pt promoted Nb-doped TiO_2 photo-catalysts: Interpreting quantum efficiency. *Appl. Catal. B Environ.* **2017**, *216*, 133–145. [CrossRef]
27. Fornari, A.M.D.; de Araujo, M.B.; Duarte, C.B.; Machado, G.; Teixeira, S.R.; Weibel, D.E. Photocatalytic reforming of aqueous formaldehyde with hydrogen generation over TiO_2 nanotubes loaded with Pt or Au nanoparticles. *Int. J. Hydrogen Energy* **2016**, *41*, 11599–11607. [CrossRef]
28. Ge, M.; Cai, J.; Iocozzia, J.; Cao, C.; Huang, J.; Zhang, X.; Shen, J.; Wang, S.; Zhang, S.; Zhang, K.-Q. A review of TiO_2 nanostructured catalysts for sustainable H_2 generation. *Int. J. Hydrogen Energy* **2017**, *42*, 8418–8449. [CrossRef]
29. Guerrero-Araque, D.; Acevedo-Peña, P.; Ramírez-Ortega, D.; Calderon, H.A.; Gómez, R. Charge transfer processes involved in photocatalytic hydrogen production over CuO/ZrO_2–TiO_2 materials. *Int. J. Hydrogen Energy* **2017**, *42*, 9744–9753. [CrossRef]
30. Gullapelli, S.; Scurrell, M.S.; Valluri, D.K. Photocatalytic H_2 production from glycerol–water mixtures over Ni/γ-Al_2O_3 and TiO_2 composite systems. *Int. J. Hydrogen Energy* **2017**, *42*, 15031–15043. [CrossRef]
31. Gupta, B.; Melvin, A.A.; Matthews, T.; Dash, S.; Tyagi, A. TiO_2 modification by gold (Au) for photocatalytic hydrogen (H_2) production. *Renew. Sustain. Energy Rev.* **2016**, *58*, 1366–1375. [CrossRef]
32. Gusain, R.; Singhal, N.; Singh, R.; Kumar, U.; Khatri, O.P. Ionic-Liquid-Functionalized Copper Oxide Nanorods for Photocatalytic Splitting of Water. *ChemPlusChem* **2016**, *81*, 489–495. [CrossRef]
33. Hashimoto, T.; Ohta, H.; Nasu, H.; Ishihara, A. Preparation and photocatalytic activity of porous Bi_2O_3 polymorphisms. *Int. J. Hydrogen Energy* **2016**, *41*, 7388–7392. [CrossRef]
34. He, G.-L.; Zhong, Y.-H.; Chen, M.-J.; Li, X.; Fang, Y.-P.; Xu, Y.-H. One-pot hydrothermal synthesis of $SrTiO_3$-reduced graphene oxide composites with enhanced photocatalytic activity for hydrogen production. *J. Mol. Catal. A Chem.* **2016**, *423*, 70–76. [CrossRef]
35. Su, J.; Zhang, T.; Wang, L.; Shi, J.; Chen, Y. Surface treatment effect on the photocatalytic hydrogen generation of CdS/ZnS core-shell microstructures. *Chin. J. Catal.* **2017**, *38*, 489–497. [CrossRef]
36. Hinojosa-Reyes, M.; Hernández-Gordillo, A.; Zanella, R.; Rodríguez-González, V. Renewable hydrogen harvest process by hydrazine as scavenging electron donor using gold TiO_2 photocatalysts. *Catal. Today* **2016**, *266*, 2–8. [CrossRef]
37. Hou, H.-J.; Zhang, X.-H.; Huang, D.-K.; Ding, X.; Wang, S.-Y.; Yang, X.-L.; Li, S.-Q.; Xiang, Y.-G.; Chen, H. Conjugated microporous poly (benzothiadiazole)/TiO_2 heterojunction for visible-light-driven H_2 production and pollutant removal. *Appl. Catal. B Environ.* **2017**, *203*, 563–571. [CrossRef]
38. Hu, J.; Wang, L.; Zhang, P.; Liang, C.; Shao, G. Construction of solid-state Z-scheme carbon-modified TiO_2/WO_3 nanofibers with enhanced photocatalytic hydrogen production. *J. Power Sources* **2016**, *328*, 28–36. [CrossRef]
39. Hu, X.; Xiao, L.; Jian, X.; Zhou, W. Synthesis of mesoporous silica-embedded TiO_2 loaded with Ag nanoparticles for photocatalytic hydrogen evolution from water splitting. *J. Wuhan Univ. Technol. Mater. Sci. Ed.* **2017**, *32*, 67–75. [CrossRef]
40. Iervolino, G.; Vaiano, V.; Sannino, D.; Rizzo, L.; Palma, V. Enhanced photocatalytic hydrogen production from glucose aqueous matrices on Ru-doped $LaFeO_3$. *Appl. Catal. B Environ.* **2017**, *207*, 182–194. [CrossRef]
41. Jeong, S.; Chung, K.-H.; Lee, H.; Park, H.; Jeon, K.-J.; Park, Y.-K.; Jung, S.-C. Enhancement of Hydrogen Evolution from Water Photocatalysis Using Liquid Phase Plasma on Metal Oxide-Loaded Photocatalysts. *ACS Sustain. Chem. Eng.* **2017**, *5*, 3659–3666. [CrossRef]

42. Jiang, C.; Lee, K.Y.; Parlett, C.M.; Bayazit, M.K.; Lau, C.C.; Ruan, Q.; Moniz, S.J.; Lee, A.F.; Tang, J. Size-controlled TiO_2 nanoparticles on porous hosts for enhanced photocatalytic hydrogen production. *Appl. Catal. A Gen.* **2016**, *521*, 133–139. [CrossRef]
43. Jiang, Q.; Li, L.; Bi, J.; Liang, S.; Liu, M. Design and Synthesis of TiO_2 Hollow Spheres with Spatially Separated Dual Cocatalysts for Efficient Photocatalytic Hydrogen Production. *Nanomaterials* **2017**, *7*, 24. [CrossRef] [PubMed]
44. Jung, M.; Hart, J.N.; Boensch, D.; Scott, J.; Ng, Y.H.; Amal, R. Hydrogen evolution via glycerol photoreforming over Cu–Pt nanoalloys on TiO_2. *Appl. Catal. A Gen.* **2016**, *518*, 221–230. [CrossRef]
45. Jung, M.; Hart, J.N.; Scott, J.; Ng, Y.H.; Jiang, Y.; Amal, R. Exploring Cu oxidation state on TiO_2 and its transformation during photocatalytic hydrogen evolution. *Appl. Catal. A Gen.* **2016**, *521*, 190–201. [CrossRef]
46. Kang, H.W.; Park, S.B. Effects of Mo sources on Mo doped $SrTiO_3$ powder prepared by spray pyrolysis for H_2 evolution under visible light irradiation. *Mater. Sci. Eng. B* **2016**, *211*, 67–74. [CrossRef]
47. Kang, H.W.; Park, S.B. Improved performance of tri-doped photocatalyst $SrTiO_3$: Rh/Ta/F for H_2 evolution under visible light irradiation. *Int. J. Hydrogen Energy* **2016**, *41*, 13970–13978. [CrossRef]
48. Khan, M.; Sinatra, L.; Oufi, M.; Bakr, O.M.; Idriss, H. Evidence of plasmonic induced photocatalytic hydrogen production on Pd/TiO_2 upon deposition on thin films of gold. *Catal. Lett.* **2017**, *147*, 811–820. [CrossRef]
49. Khore, S.K.; Tellabati, N.V.; Apte, S.K.; Naik, S.D.; Ojha, P.; Kale, B.B.; Sonawane, R.S. Green sol–gel route for selective growth of 1D rutile N–TiO_2: A highly active photocatalyst for H_2 generation and environmental remediation under natural sunlight. *RSC Adv.* **2017**, *7*, 33029–33042. [CrossRef]
50. Kim, Y.K.; Seo, H.-J.; Kim, S.; Hwang, S.-H.; Park, H.; Lim, S.K. Effect of ZnO Electrodeposited on Carbon Film and Decorated with Metal Nanoparticles for Solar Hydrogen Production. *J. Mater. Sci. Technol.* **2016**, *32*, 1059–1065. [CrossRef]
51. Kumar, D.P.; Reddy, N.L.; Karthik, M.; Neppolian, B.; Madhavan, J.; Shankar, M. Solar light sensitized p-Ag_2O/n-TiO_2 nanotubes heterojunction photocatalysts for enhanced hydrogen production in aqueous-glycerol solution. *Sol. Energy Mater. Sol. Cells* **2016**, *154*, 78–87. [CrossRef]
52. Li, C.; Wang, H.; Lu, D.; Wu, W.; Ding, J.; Zhao, X.; Xiong, R.; Yang, M.; Wu, P.; Chen, F. Visible-light-driven water splitting from dyeing wastewater using Pt surface-dispersed TiO_2-based nanosheets. *J. Alloys Compd.* **2017**, *699*, 183–192. [CrossRef]
53. Li, F.; Wangyang, P.; Zada, A.; Humayun, M.; Wang, B.; Qu, Y. Synthesis of hierarchical Mn_2O_3 microspheres for photocatalytic hydrogen production. *Mater. Res. Bull.* **2016**, *84*, 99–104. [CrossRef]
54. Li, M.; Chen, Y.; Li, W.; Li, X.; Tian, H.; Wei, X.; Ren, Z.; Han, G. Ultrathin Anatase TiO_2 Nanosheets for High-Performance Photocatalytic Hydrogen Production. *Small* **2017**, *13*, 1604115. [CrossRef]
55. Li, R.; Zhao, Y.; Li, C. Spatial distribution of active sites on a ferroelectric $PbTiO_3$ photocatalyst for photocatalytic hydrogen production. *Faraday Discuss.* **2017**, *198*, 463–472. [CrossRef]
56. Li, X.; Gao, Y.; Liu, J.; Yu, X.; Li, Z. Facile synthesis of Ti3+ doped Ag/AgI TiO_2 nanoparticles with efficient visible-light photocatalytic activity. *Int. J. Hydrogen Energy* **2017**, *42*, 13031–13038. [CrossRef]
57. Liang, J.; Chai, Y.; Li, L. Facile fabrication of rod-shaped Zn_2GeO_4 nanocrystals as photocatalyst for hydrogen production. *Cryst. Res. Technol.* **2017**, *52*, 1700022. [CrossRef]
58. Kuang, P.Y.; Zheng, P.X.; Liu, Z.Q.; Lei, J.L.; Wu, H.; Li, N.; Ma, T.Y. Embedding Au quantum dots in rimous cadmium sulfide nanospheres for enhanced photocatalytic hydrogen evolution. *Small* **2016**, *12*, 6735–6744. [CrossRef]
59. Peng, B.; Liu, X.; Li, R. Preparation of a Single-Walled Carbon Nanotube/Cd0.8Zn0.2S Nanocomposite and Its Enhanced Photocatalytic Hydrogen Production Activity. *Eur. J. Inorg. Chem.* **2016**, *2016*, 3204–3212. [CrossRef]
60. Liu, Y.; Xiong, J.; Yang, Y.; Luo, S.; Zhang, S.; Li, Y.; Liang, S.; Wu, L. HNb_xTa_{1-x} WO_6 monolayer nanosheets solid solutions: Tunable energy band structures and highly enhanced photocatalytic performances for hydrogen evolution. *Appl. Catal. B Environ.* **2017**, *203*, 798–806. [CrossRef]
61. Lozano-Sánchez, L.; Méndez-Medrano, M.; Colbeau-Justin, C.; Rodríguez-López, J.; Hernández-Uresti, D.; Obregón, S. Long-lived photoinduced charge-carriers in Er^{3+} doped $CaTiO_3$ for photocatalytic H_2 production under UV irradiation. *Catal. Commun.* **2016**, *84*, 36–39. [CrossRef]
62. Lucchetti, R.; Onotri, L.; Clarizia, L.; Di Natale, F.; Di Somma, I.; Andreozzi, R.; Marotta, R. Removal of nitrate and simultaneous hydrogen generation through photocatalytic reforming of glycerol over "in situ" prepared zero-valent nano copper/P25. *Appl. Catal. B Environ.* **2017**, *202*, 539–549. [CrossRef]

63. Luévano-Hipólito, E.; Torres-Martínez, L.; Sánchez-Martínez, D.; Cruz, M.A. Cu_2O precipitation-assisted with ultrasound and microwave radiation for photocatalytic hydrogen production. *Int. J. Hydrogen Energy* **2017**, *42*, 12997–13010. [CrossRef]
64. Luna, A.L.; Novoseltceva, E.; Louarn, E.; Beaunier, P.; Kowalska, E.; Ohtani, B.; Valenzuela, M.A.; Remita, H.; Colbeau-Justin, C. Synergetic effect of Ni and Au nanoparticles synthesized on titania particles for efficient photocatalytic hydrogen production. *Appl. Catal. B Environ.* **2016**, *191*, 18–28. [CrossRef]
65. Majeed, I.; Nadeem, M.A.; Badshah, A.; Kanodarwala, F.K.; Ali, H.; Khan, M.A.; Stride, J.A.; Nadeem, M.A. Titania supported MOF-199 derived Cu–Cu_2O nanoparticles: Highly efficient non-noble metal photocatalysts for hydrogen production from alcohol–water mixtures. *Catal. Sci. Technol.* **2017**, *7*, 677–686. [CrossRef]
66. Manjunath, K.; Souza, V.; Ramakrishnappa, T.; Nagaraju, G.; Scholten, J.; Dupont, J. Heterojunction CuO-TiO_2 nanocomposite synthesis for significant photocatalytic hydrogen production. *Mater. Res. Express* **2016**, *3*, 115904. [CrossRef]
67. Manjunath, K.; Souza, V.S.; Ganganagappa, N.; Scholten, J.D.; Teixeira, S.R.; Dupont, J.; Thippeswamy, R. Effect of the magnetic core of $(MnFe)_2O_3$@Ta_2O_5 nanoparticles on photocatalytic hydrogen production. *New J. Chem.* **2017**, *41*, 326–334. [CrossRef]
68. Mansingh, S.; Padhi, D.; Parida, K. Enhanced photocatalytic activity of nanostructured Fe doped CeO_2 for hydrogen production under visible light irradiation. *Int. J. Hydrogen Energy* **2016**, *41*, 14133–14146. [CrossRef]
69. Markovskaya, D.V.; Kozlova, E.A.; Cherepanova, S.V.; Saraev, A.A.; Gerasimov, E.Y.; Parmon, V.N. Synthesis of Pt/$Zn(OH)_2$/$Cd_{0.3}Zn_{0.7}S$ for the Photocatalytic Hydrogen Evolution from Aqueous Solutions of Organic and Inorganic Electron Donors Under Visible Light. *Top. Catal.* **2016**, *59*, 1297–1304. [CrossRef]
70. Melián, E.P.; López, C.R.; Santiago, D.E.; Quesada-Cabrera, R.; Méndez, J.O.; Rodríguez, J.D.; Díaz, O.G. Study of the photocatalytic activity of Pt-modified commercial TiO_2 for hydrogen production in the presence of common organic sacrificial agents. *Appl. Catal. A Gen.* **2016**, *518*, 189–197. [CrossRef]
71. Méndez-Medrano, M.; Kowalska, E.; Lehoux, A.; Herissan, A.; Ohtani, B.; Rau, S.; Colbeau-Justin, C.; Rodríguez-López, J.; Remita, H. Surface Modification of TiO_2 with Au Nanoclusters for Efficient Water Treatment and Hydrogen Generation under Visible Light. *J. Phys. Chem. C* **2016**, *120*, 25010–25022. [CrossRef]
72. Meng, A.; Zhang, J.; Xu, D.; Cheng, B.; Yu, J. Enhanced photocatalytic H_2-production activity of anatase TiO_2 nanosheet by selectively depositing dual-cocatalysts on {101} and {001} facets. *Appl. Catal. B Environ.* **2016**, *198*, 286–294. [CrossRef]
73. Michal, R.; Dworniczek, E.; Caplovicova, M.; Monfort, O.; Lianos, P.; Caplovic, L.; Plesch, G. Photocatalytic properties and selective antimicrobial activity of TiO_2 (Eu)/CuO nanocomposite. *Appl. Surf. Sci.* **2016**, *371*, 538–546. [CrossRef]
74. Miseki, Y.; Fujiyoshi, S.; Gunji, T.; Sayama, K. Photocatalytic Z-scheme water splitting for independent H_2/O_2 production via a stepwise operation employing a vanadate redox mediator under visible light. *J. Phys. Chem. C* **2017**, *121*, 9691–9697. [CrossRef]
75. Moon, S.Y.; Naik, B.; Park, J.Y. Photocatalytic activity of metal-decorated SiO_2@TiO_2 hybrid photocatalysts under water splitting. *Korean J. Chem. Eng.* **2016**, *33*, 2325–2329. [CrossRef]
76. Nadeem, M.A.; Al-Oufi, M.; Wahab, A.K.; Anjum, D.; Idriss, H. Hydrogen Production on Ag-Pd/TiO_2 Bimetallic Catalysts: Is there a Combined Effect of Surface Plasmon Resonance with Schottky Mechanism on the Photo-Catalytic Activity? *ChemistrySelect* **2017**, *2*, 2754–2762. [CrossRef]
77. Narendranath, S.B.; Thekkeparambil, S.V.; George, L.; Thundiyil, S.; Devi, R.N. Photocatalytic H_2 evolution from water–methanol mixtures on $InGaO_3(ZnO)$ m with an anisotropic layered structure modified with CuO and NiO cocatalysts. *J. Mol. Catal. A Chem.* **2016**, *415*, 82–88. [CrossRef]
78. Niu, F.; Shen, S.; Guo, L. A noble-metal-free artificial photosynthesis system with TiO_2 as electron relay for efficient photocatalytic hydrogen evolution. *J. Catal.* **2016**, *344*, 141–147. [CrossRef]
79. Nsib, M.F.; Saafi, S.; Rayes, A.; Moussa, N.; Houas, A. Enhanced photocatalytic performance of Ni–ZnO/Polyaniline composite for the visible-light driven hydrogen generation. *J. Energy Inst.* **2016**, *89*, 694–703. [CrossRef]
80. Obregón, S.; Lee, S.; Rodríguez-González, V. Loading effects of silver nanoparticles on hydrogen photoproduction using a Cu-TiO_2 photocatalyst. *Mater. Lett.* **2016**, *173*, 174–177. [CrossRef]
81. Pai, M.R.; Banerjee, A.M.; Rawool, S.A.; Singhal, A.; Nayak, C.; Ehrman, S.H.; Tripathi, A.K.; Bharadwaj, S.R. A comprehensive study on sunlight driven photocatalytic hydrogen generation using low cost nanocrystalline Cu-Ti oxides. *Sol. Energy Mater. Sol. Cells* **2016**, *154*, 104–120. [CrossRef]

82. Patra, K.K.; Gopinath, C.S. Bimetallic and Plasmonic Ag–Au on TiO_2 for Solar Water Splitting: An Active Nanocomposite for Entire Visible-Light-Region Absorption. *ChemCatChem* **2016**, *8*, 3294–3311. [CrossRef]
83. Pérez-Larios, A.; Hernández-Gordillo, A.; Morales-Mendoza, G.; Lartundo-Rojas, L.; Mantilla, Á.; Gómez, R. Enhancing the H_2 evolution from water–methanol solution using Mn^{2+}–Mn^{+3}–Mn^{4+} redox species of Mn-doped TiO_2 sol–gel photocatalysts. *Catal. Today* **2016**, *266*, 9–16. [CrossRef]
84. Polliotto, V.; Morra, S.; Livraghi, S.; Valetti, F.; Gilardi, G.; Giamello, E. Electron transfer and H_2 evolution in hybrid systems based on [FeFe]-hydrogenase anchored on modified TiO_2. *Int. J. Hydrogen Energy* **2016**, *41*, 10547–10556. [CrossRef]
85. Preethi, L.; Antony, R.P.; Mathews, T.; Loo, S.; Wong, L.H.; Dash, S.; Tyagi, A. Nitrogen doped anatase-rutile heterostructured nanotubes for enhanced photocatalytic hydrogen production: Promising structure for sustainable fuel production. *Int. J. Hydrogen Energy* **2016**, *41*, 5865–5877. [CrossRef]
86. Priebe, J.B.; Radnik, J.; Kreyenschulte, C.; Lennox, A.J.; Junge, H.; Beller, M.; Brückner, A. H_2 Generation with (Mixed) Plasmonic Cu/Au-TiO_2 Photocatalysts: Structure–Reactivity Relationships Assessed by in situ Spectroscopy. *ChemCatChem* **2017**, *9*, 1025–1031. [CrossRef]
87. Qiu, Y.; Ouyang, F. Fabrication of TiO_2 hierarchical architecture assembled by nanowires with anatase/TiO_2 (B) phase-junctions for efficient photocatalytic hydrogen production. *Appl. Surf. Sci.* **2017**, *403*, 691–698. [CrossRef]
88. Qiu, Y.; Ouyang, F.; Zhu, R. A facile nonaqueous route for preparing mixed-phase TiO_2 with high activity in photocatalytic hydrogen generation. *Int. J. Hydrogen Energy* **2017**, *42*, 11364–11371. [CrossRef]
89. Ramasami, A.K.; Ravishankar, T.N.; Nagaraju, G.; Ramakrishnappa, T.; Teixeira, S.R.; Balakrishna, R.G. Gel-combustion-synthesized ZnO nanoparticles for visible light-assisted photocatalytic hydrogen generation. *Bull. Mater. Sci.* **2017**, *40*, 345–354. [CrossRef]
90. Rather, R.A.; Singh, S.; Pal, B. Visible and direct sunlight induced H_2 production from water by plasmonic Ag-TiO_2 nanorods hybrid interface. *Sol. Energy Mater. Sol. Cells* **2017**, *160*, 463–469. [CrossRef]
91. Rather, R.A.; Singh, S.; Pal, B. A Cu^{+1}/Cu^0-TiO_2 mesoporous nanocomposite exhibits improved H_2 production from H_2O under direct solar irradiation. *J. Catal.* **2017**, *346*, 1–9. [CrossRef]
92. Ravishankar, T.N.; Vaz, M.D.O.; Khan, S.; Ramakrishnappa, T.; Teixeira, S.R.; Balakrishna, G.; Nagaraju, G.; Dupont, J. Ionic Liquid Assisted Hydrothermal Syntheses of TiO_2/CuO Nano-Composites for Enhanced Photocatalytic Hydrogen Production from Water. *ChemistrySelect* **2016**, *1*, 2199–2206. [CrossRef]
93. Ravishankar, T.N.; Vaz, M.D.O.; Ramakrishnappa, T.; Teixeira, S.R.; Dupont, J. Ionic liquid assisted hydrothermal syntheses of Au doped TiO_2 NPs for efficient visible-light photocatalytic hydrogen production from water, electrochemical detection and photochemical detoxification of hexavalent chromium (Cr^{6+}). *RSC Adv.* **2017**, *7*, 43233–43244. [CrossRef]
94. Reddy, N.L.; Emin, S.; Valant, M.; Shankar, M. Nanostructured Bi_2O_3@TiO_2 photocatalyst for enhanced hydrogen production. *Int. J. Hydrogen Energy* **2017**, *42*, 6627–6636. [CrossRef]
95. Reddy, P.A.K.; Manvitha, C.; Reddy, P.V.L.; Kim, K.-H.; Kumari, V.D. Enhanced hydrogen production activity over BiOX TiO_2 under solar irradiation: Improved charge transfer through bismuth oxide clusters. *J. Energy Chem.* **2017**, *26*, 390–397. [CrossRef]
96. Ren, X.; Hou, H.; Liu, Z.; Gao, F.; Zheng, J.; Wang, L.; Li, W.; Ying, P.; Yang, W.; Wu, T. Shape-Enhanced Photocatalytic Activities of Thoroughly Mesoporous ZnO Nanofibers. *Small* **2016**, *12*, 4007–4017. [CrossRef] [PubMed]
97. Rico-Oller, B.; Boudjemaa, A.; Bahruji, H.; Kebir, M.; Prashar, S.; Bachari, K.; Fajardo, M.; Gómez-Ruiz, S. Photodegradation of organic pollutants in water and green hydrogen production via methanol photoreforming of doped titanium oxide nanoparticles. *Sci. Total Environ.* **2016**, *563*, 921–932. [CrossRef] [PubMed]
98. Sadanandam, G.; Valluri, D.K.; Scurrell, M.S. Highly stabilized Ag_2O-loaded nano TiO_2 for hydrogen production from glycerol: Water mixtures under solar light irradiation. *Int. J. Hydrogen Energy* **2017**, *42*, 807–820. [CrossRef]
99. Sakata, Y.; Miyoshi, Y.; Maeda, T.; Ishikiriyama, K.; Yamazaki, Y.; Imamura, H.; Ham, Y.; Hisatomi, T.; Kubota, J.; Yamakata, A. Photocatalytic property of metal ion added $SrTiO_3$ to Overall H_2O splitting. *Appl. Catal. A Gen.* **2016**, *521*, 227–232. [CrossRef]

100. Salgado, S.Y.A.; Zamora, R.M.R.; Zanella, R.; Peral, J.; Malato, S.; Maldonado, M.I. Photocatalytic hydrogen production in a solar pilot plant using a Au/TiO_2 photo catalyst. *Int. J. Hydrogen Energy* **2016**, *41*, 11933–11940. [CrossRef]
101. Sampaio, M.J.; Oliveira, J.W.; Sombrio, C.I.; Baptista, D.L.; Teixeira, S.R.; Carabineiro, S.A.; Silva, C.G.; Faria, J.L. Photocatalytic performance of Au/ZnO nanocatalysts for hydrogen production from ethanol. *Appl. Catal. A Gen.* **2016**, *518*, 198–205. [CrossRef]
102. Siddiqi, G.; Mougel, V.; Copéret, C. Highly Active Subnanometer Au Particles Supported on TiO_2 for Photocatalytic Hydrogen Evolution from a Well-Defined Organogold Precursor, [Au_5(mesityl)$_5$]. *Inorg. Chem.* **2016**, *55*, 4026–4033. [CrossRef]
103. Song, T.; Zhang, P.; Zeng, J.; Wang, T.; Ali, A.; Zeng, H. Boosting the photocatalytic H_2 evolution activity of Fe_2O_3 polymorphs (α-, γ-and β-Fe_2O_3) by fullerene [C_{60}]-modification and dye-sensitization under visible light irradiation. *RSC Adv.* **2017**, *7*, 29184–29192. [CrossRef]
104. Sun, X.; Wang, S.; Shen, C.; Xu, X. Efficient Photocatalytic Hydrogen Production over Rh-Doped Inverse Spinel Zn_2TiO_4. *ChemCatChem* **2016**, *8*, 2289–2295. [CrossRef]
105. Taylor, S.; Mehta, M.; Barbash, D.; Samokhvalov, A. One-pot photoassisted synthesis, in situ photocatalytic testing for hydrogen generation and the mechanism of binary nitrogen and copper promoted titanium dioxide. *Photochem. Photobiol. Sci.* **2017**, *16*, 916–924. [CrossRef]
106. Tian, H.; Wang, S.; Zhang, C.; Veder, J.-P.; Pan, J.; Jaroniec, M.; Wang, L.; Liu, J. Design and synthesis of porous $ZnTiO_3$/TiO_2 nanocages with heterojunctions for enhanced photocatalytic H_2 production. *J. Mater. Chem. A* **2017**, *5*, 11615–11622. [CrossRef]
107. Tiwari, A.; Mondal, I.; Ghosh, S.; Chattopadhyay, N.; Pal, U. Fabrication of mixed phase TiO_2 heterojunction nanorods and their enhanced photoactivities. *Phys. Chem. Chem. Phys.* **2016**, *18*, 15260–15268. [CrossRef] [PubMed]
108. Vebber, M.; Faria, A.; Dal'Acqua, N.; Beal, L.; Fetter, G.; Machado, G.; Giovanela, M.; Crespo, J. Hydrogen production by photocatalytic water splitting using poly (allylamine hydrochloride)/poly (acrylic acid)/TiO_2/copper chlorophyllin self-assembled thin films. *Int. J. Hydrogen Energy* **2016**, *41*, 17995–18004. [CrossRef]
109. Wang, C.; Cai, X.; Chen, Y.; Cheng, Z.; Lin, P.; Yang, Z.; Sun, S. Improved Hydrogen Production by Glycerol Photoreforming over Ag_2O-TiO_2 Nanocomposite Mixed Oxide Synthesized by a Sol-gel Method. *Energy Procedia* **2017**, *105*, 1657–1664. [CrossRef]
110. Wang, P.; Sun, F.; Kim, J.H.; Kim, J.H.; Yang, J.; Wang, X.; Lee, J.S. Synthesis of high-purity, layered structured $K_2Ta_4O_{11}$ intermediate phase nanocrystals for photocatalytic water splitting. *Phys. Chem. Chem. Phys.* **2016**, *18*, 25831–25836. [CrossRef]
111. Wang, Q.; Jiao, D.; Wu, Y.; Guo, H.; She, H.; Li, J.; Zhong, J.; Wang, F.; Tong, J. Carbon doped solid solution $Bi_{0.5}Dy_{0.5}VO_4$ for efficient photocatalytic hydrogen evolution from water. *Int. J. Hydrogen Energy* **2016**, *41*, 16032–16039. [CrossRef]
112. Wang, M.; Shen, S.; Li, L.; Tang, Z.; Yang, J. Effects of sacrificial reagents on photocatalytic hydrogen evolution over different photocatalysts. *J. Mater. Sci.* **2017**, *52*, 5155–5164. [CrossRef]
113. Song, Y.; Wei, S.; Rong, Y.; Lu, C.; Chen, Y.; Wang, J.; Zhang, Z. Enhanced visible-light photocatalytic hydrogen evolution activity of Er^{3+}:$Y_3Al_5O_{12}$/PdS–ZnS by conduction band co-catalysts (MoO_2, MoS_2 and $MoSe_2$). *Int. J. Hydrogen Energy* **2016**, *41*, 12826–12835. [CrossRef]
114. Zhang, K.; Qian, S.; Kim, W.; Kim, J.K.; Sheng, X.; Lee, J.Y.; Park, J.H. Double 2-dimensional H_2-evoluting catalyst tipped photocatalyst nanowires: A new avenue for high-efficiency solar to H_2 generation. *Nano Energy* **2017**, *34*, 481–490. [CrossRef]
115. Wu, B.-H.; Liu, W.-T.; Chen, T.-Y.; Perng, T.-P.; Huang, J.-H.; Chen, L.-J. Plasmon-enhanced photocatalytic hydrogen production on Au/TiO_2 hybrid nanocrystal arrays. *Nano Energy* **2016**, *27*, 412–419. [CrossRef]
116. Xie, S.; Wang, Z.; Cheng, F.; Zhang, P.; Mai, W.; Tong, Y. Ceria and ceria-based nanostructured materials for photoenergy applications. *Nano Energy* **2017**, *34*, 313–337. [CrossRef]
117. Xiong, J.; Liu, Y.; Liang, S.; Zhang, S.; Li, Y.; Wu, L. Insights into the role of Cu in promoting photocatalytic hydrogen production over ultrathin HNb_3O_8 nanosheets. *J. Catal.* **2016**, *342*, 98–104. [CrossRef]
118. Xu, D.; Hai, Y.; Zhang, X.; Zhang, S.; He, R. Bi_2O_3 cocatalyst improving photocatalytic hydrogen evolution performance of TiO_2. *Appl. Surf. Sci.* **2017**, *400*, 530–536. [CrossRef]

119. Liu, H.; Xu, Z.; Zhang, Z.; Ao, D. Highly efficient photocatalytic H_2 evolution from water over $CdLa_2S_4$/mesoporous gC_3N_4 hybrids under visible light irradiation. *Appl. Catal. B Environ.* **2016**, *192*, 234–241. [CrossRef]
120. Xu, L.; Sun, X.; Tu, H.; Jia, Q.; Gong, H.; Guan, J. Synchronous etching-epitaxial growth fabrication of facet-coupling $NaTaO_3/Ta_2O_5$ heterostructured nanofibers for enhanced photocatalytic hydrogen production. *Appl. Catal. B Environ.* **2016**, *184*, 309–319. [CrossRef]
121. Xu, X.; Lv, M.; Sun, X.; Liu, G. Role of surface composition upon the photocatalytic hydrogen production of Cr-doped and La/Cr-codoped $SrTiO_3$. *J. Mater. Sci.* **2016**, *51*, 6464–6473. [CrossRef]
122. Yan, X.; Xue, C.; Yang, B.; Yang, G. Novel three-dimensionally ordered macroporous Fe^{3+}-doped TiO_2 photocatalysts for H_2 production and degradation applications. *Appl. Surf. Sci.* **2017**, *394*, 248–257. [CrossRef]
123. Yang, Y.; Gao, P.; Wang, Y.; Sha, L.; Ren, X.; Zhang, J.; Yang, P.; Wu, T.; Chen, Y.; Li, X. A simple and efficient hydrogen production-storage hybrid system (Co/TiO_2) for synchronized hydrogen photogeneration with uptake. *J. Mater. Chem. A* **2017**, *5*, 9198–9203. [CrossRef]
124. Yang, Y.; Liu, G.; Irvine, J.T.; Cheng, H.M. Enhanced Photocatalytic H_2 Production in Core–Shell Engineered Rutile TiO_2. *Adv. Mater.* **2016**, *28*, 5850–5856. [CrossRef] [PubMed]
125. Yao, Z.; Zhang, Y.; He, Y.; Xia, Q.; Jiang, Z. Synthesis of hierarchical dendritic micro–nano structure $ZnFe_2O_4$ and photocatalytic activities for water splitting. *Chin. J. Chem. Eng.* **2016**, *24*, 1112–1116. [CrossRef]
126. Yu, H.; Sun, D.; Liu, J.; Fang, Y.; Li, C.C. Monodisperse mesoporous Ta_2O_5 colloidal spheres as a highly effective photocatalyst for hydrogen production. *Int. J. Hydrogen Energy* **2016**, *41*, 17225–17232. [CrossRef]
127. Yu, X.; Wei, Y.; Li, Z.; Liu, J. One-step synthesis of the single crystal Ta_2O_5 nanowires with superior hydrogen production activity. *Mater. Lett.* **2017**, *191*, 150–153. [CrossRef]
128. Ma, C.; Zhu, H.; Zhou, J.; Cui, Z.; Liu, T.; Wang, Y.; Wang, Y.; Zou, Z. Confinement effect of monolayer MoS_2 quantum dots on conjugated polyimide and promotion of solar-driven photocatalytic hydrogen generation. *Dalton Trans.* **2017**, *46*, 3877–3886. [CrossRef] [PubMed]
129. Zhang, J.; Yu, Z.; Gao, Z.; Ge, H.; Zhao, S.; Chen, C.; Chen, S.; Tong, X.; Wang, M.; Zheng, Z. Porous TiO_2 nanotubes with spatially separated platinum and CoOx cocatalysts produced by atomic layer deposition for photocatalytic hydrogen production. *Angew. Chem. Int. Ed.* **2017**, *56*, 816–820. [CrossRef]
130. Zhang, M.; Sun, R.; Li, Y.; Shi, Q.; Xie, L.; Chen, J.; Xu, X.; Shi, H.; Zhao, W. High H_2 evolution from quantum Cu (II) nanodot-doped two-dimensional ultrathin TiO_2 nanosheets with dominant exposed {001} facets for reforming glycerol with multiple electron transport pathways. *J. Phys. Chem. C* **2016**, *120*, 10746–10756. [CrossRef]
131. Zhang, Q.; Li, R.; Li, Z.; Li, A.; Wang, S.; Liang, Z.; Liao, S.; Li, C. The dependence of photocatalytic activity on the selective and nonselective deposition of noble metal cocatalysts on the facets of rutile TiO_2. *J. Catal.* **2016**, *337*, 36–44. [CrossRef]
132. Zhang, Y.J.; Zhang, L.; Kang, L.; Yang, M.Y.; Zhang, K. A new $CaWO_4$/alkali-activated blast furnace slag-based cementitious composite for production of hydrogen. *Int. J. Hydrogen Energy* **2017**, *42*, 3690–3697. [CrossRef]
133. Shen, C.-C.; Liu, Y.-N.; Zhou, X.; Guo, H.-L.; Zhao, Z.-W.; Liang, K.; Xu, A.-W. Large improvement of visible-light photocatalytic H_2-evolution based on cocatalyst-free $Zn_{0.5}Cd_{0.5}S$ synthesized through a two-step process. *Catal. Sci. Technol.* **2017**, *7*, 961–967. [CrossRef]
134. Zhu, F.; Li, C.; Ha, M.N.; Liu, Z.; Guo, Q.; Zhao, Z. Molten-salt synthesis of Cu–$SrTiO_3/TiO_2$ nanotube heterostructures for photocatalytic water splitting. *J. Mater. Sci.* **2016**, *51*, 4639–4649. [CrossRef]
135. Zhu, M.; Cai, X.; Fujitsuka, M.; Zhang, J.; Majima, T. Au/$La_2Ti_2O_7$ Nanostructures Sensitized with Black Phosphorus for Plasmon-Enhanced Photocatalytic Hydrogen Production in Visible and Near-Infrared Light. *Angew. Chem.* **2017**, *129*, 2096–2100. [CrossRef]
136. Zhu, W.; Han, D.; Niu, L.; Wu, T.; Guan, H. Z-scheme Si/$MgTiO_3$ porous heterostructures: Noble metal and sacrificial agent free photocatalytic hydrogen evolution. *Int. J. Hydrogen Energy* **2016**, *41*, 14713–14720. [CrossRef]
137. Zhu, Z.; Kao, C.-T.; Tang, B.-H.; Chang, W.-C.; Wu, R.-J. Efficient hydrogen production by photocatalytic water-splitting using Pt-doped TiO_2 hollow spheres under visible light. *Ceram. Int.* **2016**, *42*, 6749–6754. [CrossRef]

138. Zhuang, B.; Xiangqing, L.; Ge, R.; Kang, S.; Qin, L.; Li, G. Assembly and electron transfer mechanisms on visible light responsive 5, 10, 15, 20-meso-tetra (4-carboxyphenyl) porphyrin/cuprous oxide composite for photocatalytic hydrogen production. *Appl. Catal. A Gen.* **2017**, *533*, 81–89. [CrossRef]
139. Zhuang, H.; Zhang, Y.; Chu, Z.; Long, J.; An, X.; Zhang, H.; Lin, H.; Zhang, Z.; Wang, X. Synergy of metal and nonmetal dopants for visible-light photocatalysis: A case-study of Sn and N co-doped TiO_2. *Phys. Chem. Chem. Phys.* **2016**, *18*, 9636–9644. [CrossRef] [PubMed]
140. Zywitzki, D.; Jing, H.; Tüysüz, H.; Chan, C.K. High surface area, amorphous titania with reactive Ti 3+ through a photo-assisted synthesis method for photocatalytic H_2 generation. *J. Mater. Chem. A* **2017**, *5*, 10957–10967. [CrossRef]
141. Bharatvaj, J.; Preethi, V.; Kanmani, S. Hydrogen production from sulphide wastewater using Ce^{3+}–TiO_2 photocatalysis. *Int. J. Hydrogen Energy* **2018**, *43*, 3935–3945. [CrossRef]
142. Yasuda, M.; Matsumoto, T.; Yamashita, T. Sacrificial hydrogen production over TiO_2-based photocatalysts: Polyols, carboxylic acids, and saccharides. *Renew. Sustain. Energy Rev.* **2018**, *81*, 1627–1635. [CrossRef]
143. Maldonado, M.; López-Martín, A.; Colón, G.; Peral, J.; Martínez-Costa, J.; Malato, S. Solar pilot plant scale hydrogen generation by irradiation of Cu/TiO_2 composites in presence of sacrificial electron donors. *Appl. Catal. B Environ.* **2018**, *229*, 15–23. [CrossRef]
144. Hainer, A.S.; Hodgins, J.S.; Sandre, V.; Vallieres, M.; Lanterna, A.E.; Scaiano, J.C. Photocatalytic Hydrogen Generation Using Metal-Decorated TiO_2: Sacrificial Donors vs True Water Splitting. *ACS Energy Lett.* **2018**, *3*, 542–545. [CrossRef]
145. Ravi, P.; Rao, V.N.; Shankar, M.; Sathish, M. $CuOCr_2O_3$ core-shell structured co-catalysts on TiO_2 for efficient photocatalytic water splitting using direct solar light. *Int. J. Hydrogen Energy* **2018**, *43*, 3976–3987. [CrossRef]
146. Camacho, S.Y.T.; Rey, A.; Hernández-Alonso, M.D.; Llorca, J.; Medina, F.; Contreras, S. Pd/TiO_2-WO_3 photocatalysts for hydrogen generation from water-methanol mixtures. *Appl. Surf. Sci.* **2018**, *455*, 570–580. [CrossRef]
147. Huang, J.; Li, G.; Zhou, Z.; Jiang, Y.; Hu, Q.; Xue, C.; Guo, W. Efficient photocatalytic hydrogen production over Rh and Nb codoped TiO_2 nanorods. *Chem. Eng. J.* **2018**, *337*, 282–289. [CrossRef]
148. Li, Y.; Kuang, L.; Xiao, D.; Badireddy, A.R.; Hu, M.; Zhuang, S.; Wang, X.; Lee, E.S.; Marhaba, T.; Zhang, W. Hydrogen production from organic fatty acids using carbon-doped TiO_2 nanoparticles under visible light irradiation. *Int. J. Hydrogen Energy* **2018**, *43*, 4335–4346. [CrossRef]
149. Castañeda, C.; Tzompantzi, F.; Rodríguez-Rodríguez, A.; Sánchez-Dominguez, M.; Gómez, R. Improved photocatalytic hydrogen production from methanol/water solution using CuO supported on fluorinated TiO_2. *J. Chem. Technol. Biotechnol.* **2018**, *93*, 1113–1120. [CrossRef]
150. Cai, X.; Zhang, J.; Fujitsuka, M.; Majima, T. Graphitic-C_3N_4 hybridized N-doped $La_2Ti_2O_7$ two-dimensional layered composites as efficient visible-light-driven photocatalyst. *Appl. Catal. B Environ.* **2017**, *202*, 191–198. [CrossRef]
151. Cao, S.; Jiang, J.; Zhu, B.; Yu, J. Shape-dependent photocatalytic hydrogen evolution activity over a Pt nanoparticle coupled gC_3N_4 photocatalyst. *Phys. Chem. Chem. Phys.* **2016**, *18*, 19457–19463. [CrossRef]
152. Cao, S.; Yu, J. Carbon-based H_2-production photocatalytic materials. *J. Photochem. Photobiol. C Photochem. Rev.* **2016**, *27*, 72–99. [CrossRef]
153. Chang, D.W.; Baek, J.B. Nitrogen-Doped Graphene for Photocatalytic Hydrogen Generation. *Chem. Asian J.* **2016**, *11*, 1125–1137. [CrossRef]
154. Chen, F.; Yang, H.; Wang, X.; Yu, H. Facile synthesis and enhanced photocatalytic H_2-evolution performance of NiS_2-modified gC_3N_4 photocatalysts. *Chin. J. Catal.* **2017**, *38*, 296–304. [CrossRef]
155. Chen, L.; Zhou, X.; Jin, B.; Luo, J.; Xu, X.; Zhang, L.; Hong, Y. Heterojunctions in gC_3N_4/B-TiO_2 nanosheets with exposed {001} plane and enhanced visible-light photocatalytic activities. *Int. J. Hydrogen Energy* **2016**, *41*, 7292–7300. [CrossRef]
156. Chen, L.-C.; Yeh, T.-F.; Lee, Y.-L.; Teng, H. Incorporating nitrogen-doped graphene oxide dots with graphene oxide sheets for stable and effective hydrogen production through photocatalytic water decomposition. *Appl. Catal. A Gen.* **2016**, *521*, 118–124. [CrossRef]
157. Chen, T.; Quan, W.; Yu, L.; Hong, Y.; Song, C.; Fan, M.; Xiao, L.; Gu, W.; Shi, W. One-step synthesis and visible-light-driven H_2 production from water splitting of Ag quantum dots/gC_3N_4 photocatalysts. *J. Alloys Compd.* **2016**, *686*, 628–634. [CrossRef]

158. Chen, X.; Chen, H.; Guan, J.; Zhen, J.; Sun, Z.; Du, P.; Lu, Y.; Yang, S. A facile mechanochemical route to a covalently bonded graphitic carbon nitride (gC_3N_4) and fullerene hybrid toward enhanced visible light photocatalytic hydrogen production. *Nanoscale* **2017**, *9*, 5615–5623. [CrossRef]
159. Cheng, C.; Shi, J.; Hu, Y.; Guo, L. WO_3/g-C_3N_4 composites: One-pot preparation and enhanced photocatalytic H_2 production under visible-light irradiation. *Nanotechnology* **2017**, *28*, 164002. [CrossRef]
160. Cheng, R.; Zhang, L.; Fan, X.; Wang, M.; Li, M.; Shi, J. One-step construction of FeO_x modified gC_3N_4 for largely enhanced visible-light photocatalytic hydrogen evolution. *Carbon* **2016**, *101*, 62–70. [CrossRef]
161. Gao, J.; Wang, Y.; Zhou, S.; Lin, W.; Kong, Y. A Facile One-Step Synthesis of Fe-Doped g-C_3N_4 Nanosheets and Their Improved Visible-Light Photocatalytic Performance. *ChemCatChem* **2017**, *9*, 1708–1715. [CrossRef]
162. Gholipour, M.R.; Béland, F.; Do, T.-O. Graphitic Carbon Nitride-Titanium Dioxide Nanocomposite for Photocatalytic Hydrogen Production under Visible Light. *Int. J. Chem. React. Eng.* **2016**, *14*, 851–858. [CrossRef]
163. Wenderich, K.; Mul, G. Methods, mechanism, and applications of photodeposition in photocatalysis: A review. *Chem. Rev.* **2016**, *116*, 14587–14619. [CrossRef]
164. Li, X.; Guo, S.; Kan, C.; Zhu, J.; Tong, T.; Ke, S.; Choy, W.C.; Wei, B. Au Multimer@ MoS_2 hybrid structures for efficient photocatalytical hydrogen production via strongly plasmonic coupling effect. *Nano Energy* **2016**, *30*, 549–558. [CrossRef]
165. Han, Q.; Wang, B.; Gao, J.; Qu, L. Graphitic Carbon Nitride/Nitrogen-Rich Carbon Nanofibers: Highly Efficient Photocatalytic Hydrogen Evolution without Cocatalysts. *Angew. Chem.* **2016**, *128*, 11007–11011. [CrossRef]
166. Hao, R.; Guo, S.; Wang, X.; Feng, T.; Feng, Q.; Li, M.; Jiang, B. Two-dimensional assembly structure of graphene and TiO_2 nanosheets from titanic acid with enhanced visible-light photocatalytic performance. *Chem. Phys. Lett.* **2016**, *653*, 190–195. [CrossRef]
167. Han, W.; Li, Z.; Li, Y.; Fan, X.; Zhang, F.; Zhang, G.; Peng, W. The Promoting Role of Different Carbon Allotropes Cocatalysts for Semiconductors in Photocatalytic Energy Generation and Pollutants Degradation. *Front. Chem.* **2017**, *5*, 84. [CrossRef]
168. He, K.; Xie, J.; Yang, Z.; Shen, R.; Fang, Y.; Ma, S.; Chen, X.; Li, X. Earth-abundant WC nanoparticles as an active noble-metal-free co-catalyst for the highly boosted photocatalytic H_2 production over gC_3N_4 nanosheets under visible light. *Catal. Sci. Technol.* **2017**, *7*, 1193–1202. [CrossRef]
169. Chen, Y.; He, J.; Li, J.; Mao, M.; Yan, Z.; Wang, W.; Wang, J. Hydrilla derived $ZnIn_2S_4$ photocatalyst with hexagonal-cubic phase junctions: A bio-inspired approach for H_2 evolution. *Catal. Commun.* **2016**, *87*, 1–5. [CrossRef]
170. Hong, Y.; Fang, Z.; Yin, B.; Luo, B.; Zhao, Y.; Shi, W.; Li, C. A visible-light-driven heterojunction for enhanced photocatalytic water splitting over Ta_2O_5 modified gC_3N_4 photocatalyst. *Int. J. Hydrogen Energy* **2017**, *42*, 6738–6745. [CrossRef]
171. Huang, Q.-Z.; Wang, J.-C.; Wang, P.-P.; Yao, H.-C.; Li, Z.-J. In-situ growth of mesoporous Nb_2O_5 microspheres on gC_3N_4 nanosheets for enhanced photocatalytic H_2 evolution under visible light irradiation. *Int. J. Hydrogen Energy* **2017**, *42*, 6683–6694. [CrossRef]
172. Huo, J.; Liu, X.; Li, X.; Qin, L.; Kang, S.-Z. An efficient photocatalytic system containing Eosin Y, 3D mesoporous graphene assembly and CuO for visible-light-driven H_2 evolution from water. *Int. J. Hydrogen Energy* **2017**, *42*, 15540–15550. [CrossRef]
173. Kalyani, R.; Gurunathan, K. PTh-rGO-TiO_2 nanocomposite for photocatalytic hydrogen production and dye degradation. *J. Photochem. Photobiol. A Chem.* **2016**, *329*, 105–112. [CrossRef]
174. Karthik, P.; Vinoth, R.; Selvam, P.; Balaraman, E.; Navaneethan, M.; Hayakawa, Y.; Neppolian, B. A visible-light active catechol–metal oxide carbonaceous polymeric material for enhanced photocatalytic activity. *J. Mater. Chem. A* **2017**, *5*, 384–396. [CrossRef]
175. Lau, V.W.H.; Klose, D.; Kasap, H.; Podjaski, F.; Pignié, M.C.; Reisner, E.; Jeschke, G.; Lotsch, B.V. Dark Photocatalysis: Storage of Solar Energy in Carbon Nitride for Time-Delayed Hydrogen Generation. *Angew. Chem. Int. Ed.* **2017**, *56*, 510–514. [CrossRef]
176. Lei, Y.; Shi, Q.; Han, C.; Wang, B.; Wu, N.; Wang, H.; Wang, Y. N-doped graphene grown on silk cocoon-derived interconnected carbon fibers for oxygen reduction reaction and photocatalytic hydrogen production. *Nano Res.* **2016**, *9*, 2498–2509. [CrossRef]

177. Litke, A.; Weber, T.; Hofmann, J.P.; Hensen, E.J. Bottlenecks limiting efficiency of photocatalytic water reduction by mixed Cd-Zn sulfides/Pt-TiO_2 composites. *Appl. Catal. B Environ.* **2016**, *198*, 16–24. [CrossRef]
178. Liu, B.; Su, S.; Zhou, W.; Wang, Y.; Wei, D.; Yao, L.; Ni, Y.; Cao, M.; Hu, C. Photo-reduction assisted synthesis of W-doped TiO_2 coupled with Au nanoparticles for highly efficient photocatalytic hydrogen evolution. *CrystEngComm* **2017**, *19*, 675–683. [CrossRef]
179. Liu, G.; Zhao, G.; Zhou, W.; Liu, Y.; Pang, H.; Zhang, H.; Hao, D.; Meng, X.; Li, P.; Kako, T. In situ bond modulation of graphitic carbon nitride to construct p–n homojunctions for enhanced photocatalytic hydrogen production. *Adv. Funct. Mater.* **2016**, *26*, 6822–6829. [CrossRef]
180. Lu, Y.; Ma, B.; Yang, Y.; Huang, E.; Ge, Z.; Zhang, T.; Zhang, S.; Li, L.; Guan, N.; Ma, Y. High activity of hot electrons from bulk 3D graphene materials for efficient photocatalytic hydrogen production. *Nano Res.* **2017**, *10*, 1662–1672. [CrossRef]
181. Ma, B.; Xu, H.; Lin, K.; Li, J.; Zhan, H.; Liu, W.; Li, C. Mo_2C as Non-Noble Metal Co-Catalyst in Mo_2C/CdS Composite for Enhanced Photocatalytic H_2 Evolution under Visible Light Irradiation. *ChemSusChem* **2016**, *9*, 820–824. [CrossRef]
182. Mao, Z.; Chen, J.; Yang, Y.; Wang, D.; Bie, L.; Fahlman, B.D. Novel g-C_3N_4/CoO nanocomposites with significantly enhanced visible-light photocatalytic activity for H_2 evolution. *ACS Appl. Mater. Interfaces* **2017**, *9*, 12427–12435. [CrossRef] [PubMed]
183. Mateo, D.; Esteve-Adell, I.; Albero, J.; Royo, J.F.S.; Primo, A.; Garcia, H. 111 oriented gold nanoplatelets on multilayer graphene as visible light photocatalyst for overall water splitting. *Nat. Commun.* **2016**, *7*, 11819. [CrossRef] [PubMed]
184. Mehta, A.; Pooja, D.; Thakur, A.; Basu, S. Enhanced photocatalytic water splitting by gold carbon dot core shell nanocatalyst under visible/sunlight. *New J. Chem.* **2017**, *41*, 4573–4581. [CrossRef]
185. Nguyen, C.C.; Vu, N.N.; Chabot, S.; Kaliaguine, S.; Do, T.O. Role of CxNy-Triazine in Photocatalysis for Efficient Hydrogen Generation and Organic Pollutant Degradation Under Solar Light Irradiation. *Sol. RRL* **2017**, *1*, 1700012. [CrossRef]
186. Xing, Z.; Zhang, J.; Cui, J.; Yin, J.; Zhao, T.; Kuang, J.; Xiu, Z.; Wan, N.; Zhou, W. Recent advances in floating TiO_2-based photocatalysts for environmental application. *Appl. Catal. B Environ.* **2018**, *225*, 452–467. [CrossRef]
187. Pan, Z.; Zheng, Y.; Guo, F.; Niu, P.; Wang, X. Decorating CoP and Pt nanoparticles on graphitic carbon nitride nanosheets to promote overall water splitting by conjugated polymers. *ChemSusChem* **2017**, *10*, 87–90. [CrossRef]
188. Putri, L.K.; Ng, B.-J.; Ong, W.-J.; Lee, H.W.; Chang, W.S.; Chai, S.-P. Heteroatom nitrogen-and boron-doping as a facile strategy to improve photocatalytic activity of standalone reduced graphene oxide in hydrogen evolution. *ACS Appl. Mater. Interfaces* **2017**, *9*, 4558–4569. [CrossRef]
189. Qiao, S.; Mitchell, R.W.; Coulson, B.; Jowett, D.V.; Johnson, B.R.; Brydson, R.; Isaacs, M.; Lee, A.F.; Douthwaite, R.E. Pore confinement effects and stabilization of carbon nitride oligomers in macroporous silica for photocatalytic hydrogen production. *Carbon* **2016**, *106*, 320–329. [CrossRef]
190. Qu, A.; Xu, X.; Xie, H.; Zhang, Y.; Li, Y.; Wang, J. Effects of calcining temperature on photocatalysis of gC_3N_4/TiO_2 composites for hydrogen evolution from water. *Mater. Res. Bull.* **2016**, *80*, 167–176. [CrossRef]
191. Raevskaya, A.E.; Panasiuk, Y.V.; Korzhak, G.V.; Stroyuk, O.L.; Kuchmiy, S.Y.; Dzhagan, V.M.; Zahn, D.R. Photocatalytic H_2 production from aqueous solutions of hydrazine and its derivatives in the presence of nitric-acid-activated graphitic carbon nitride. *Catal. Today* **2017**, *284*, 229–235. [CrossRef]
192. Rather, R.A.; Singh, S.; Pal, B. Core–shell morphology of Au-TiO_2@ graphene oxide nanocomposite exhibiting enhanced hydrogen production from water. *J. Ind. Eng. Chem.* **2016**, *37*, 288–294. [CrossRef]
193. She, X.; Liu, L.; Ji, H.; Mo, Z.; Li, Y.; Huang, L.; Du, D.; Xu, H.; Li, H. Template-free synthesis of 2D porous ultrathin nonmetal-doped gC_3N_4 nanosheets with highly efficient photocatalytic H_2 evolution from water under visible light. *Appl. Catal. B Environ.* **2016**, *187*, 144–153. [CrossRef]
194. Shen, L.; Xing, Z.; Zou, J.; Li, Z.; Wu, X.; Zhang, Y.; Zhu, Q.; Yang, S.; Zhou, W. Black TiO_2 nanobelts/g-C_3N_4 nanosheets Laminated Heterojunctions with Efficient Visible-Light-Driven Photocatalytic Performance. *Sci. Rep.* **2017**, *7*, 41978. [CrossRef] [PubMed]
195. Chen, Y.; Lu, C.; Tang, L.; Wei, S.; Song, Y.; Wang, J. Efficient photocatalytic hydrogen evolution from methanol/water splitting over Tm^{3+}, Yb^{3+}:$NaYF_4$–Er^{3+}:$Y_3Al_5O_{12}$/MoS_2–$NaTaO_3$ nanocomposite particles under infrared–visible light irradiation. *Sol. Energy Mater. Sol. Cells* **2016**, *149*, 128–136. [CrossRef]

196. Shin, S.R.; Park, J.H.; Kim, K.-H.; Choi, K.M.; Kang, J.K. Network of Heterogeneous Catalyst Arrays on the Nitrogen-Doped Graphene for Synergistic Solar Energy Harvesting of Hydrogen from Water. *Chem. Mater.* **2016**, *28*, 7725–7730. [CrossRef]
197. Song, K.; Xiao, F.; Zhang, L.; Yue, F.; Liang, X.; Wang, J.; Su, X. $W_{18}O_{49}$ nanowires grown on gC_3N_4 sheets with enhanced photocatalytic hydrogen evolution activity under visible light. *J. Mol. Catal. A Chem.* **2016**, *418*, 95–102. [CrossRef]
198. Sun, J.; Schmidt, B.V.; Wang, X.; Shalom, M. Self-Standing Carbon Nitride-Based Hydrogels with High Photocatalytic Activity. *ACS Appl. Mater. Interfaces* **2017**, *9*, 2029–2034. [CrossRef]
199. Sun, Q.; Wang, P.; Yu, H.; Wang, X. In situ hydrothermal synthesis and enhanced photocatalytic H_2-evolution performance of suspended rGO/gC_3N_4 photocatalysts. *J. Mol. Catal. A Chem.* **2016**, *424*, 369–376. [CrossRef]
200. Tay, Q.; Wang, X.; Zhao, X.; Hong, J.; Zhang, Q.; Xu, R.; Chen, Z. Enhanced visible light hydrogen production via a multiple heterojunction structure with defect-engineered gC_3N_4 and two-phase anatase/brookite TiO_2. *J. Catal.* **2016**, *342*, 55–62. [CrossRef]
201. Thaweesak, S.; Lyu, M.; Peerakiatkhajohn, P.; Butburee, T.; Luo, B.; Chen, H.; Wang, L. Two-dimensional $gC_3N_4/Ca_2Nb_2TaO_{10}$ nanosheet composites for efficient visible light photocatalytic hydrogen evolution. *Appl. Catal. B Environ.* **2017**, *202*, 184–190. [CrossRef]
202. Virca, C.N.; Winter, H.; Goforth, A.M.; Mackiewicz, M.R.; McCormick, T.M. Photocatalytic water reduction using a polymer coated carbon quantum dot sensitizer and a nickel nanoparticle catalyst. *Nanotechnology* **2017**, *28*, 195402. [CrossRef]
203. Zheng, D.; Zhang, G.; Hou, Y.; Wang, X. Layering MoS_2 on soft hollow gC_3N_4 nanostructures for photocatalytic hydrogen evolution. *Appl. Catal. A Gen.* **2016**, *521*, 2–8. [CrossRef]
204. Wang, J.; Feng, K.; Chen, B.; Li, Z.-J.; Meng, Q.-Y.; Zhang, L.-P.; Tung, C.-H.; Wu, L.-Z. Polymer-modified hydrophilic graphene: A promotor to photocatalytic hydrogen evolution for in situ formation of core@ shell cobalt nanocomposites. *J. Photochem. Photobiol. A Chem.* **2016**, *331*, 247–254. [CrossRef]
205. Wang, N.; Li, J.; Wu, L.; Li, X.; Shu, J. MnO_2 and carbon nanotube co-modified C_3N_4 composite catalyst for enhanced water splitting activity under visible light irradiation. *Int. J. Hydrogen Energy* **2016**, *41*, 22743–22750. [CrossRef]
206. Wang, P.; Sinev, I.; Sun, F.; Li, H.; Wang, D.; Li, Q.; Wang, X.; Marschall, R.; Wark, M. Rational fabrication of a graphitic-$C_3N_4/Sr_2KNb_5O_{15}$ nanorod composite with enhanced visible-light photoactivity for degradation of methylene blue and hydrogen production. *RSC Adv.* **2017**, *7*, 42774–42782. [CrossRef]
207. Boyjoo, Y.; Sun, H.; Liu, J.; Pareek, V.K.; Wang, S. A review on photocatalysis for air treatment: From catalyst development to reactor design. *Chem. Eng. J.* **2017**, *310*, 537–559. [CrossRef]
208. Wang, Q.; Lian, J.; Ma, Q.; Zhang, S.; He, J.; Zhong, J.; Li, J.; Huang, H.; Su, B. Preparation of carbon spheres supported CdS photocatalyst for enhancement its photocatalytic H_2 evolution. *Catal. Today* **2017**, *281*, 662–668. [CrossRef]
209. Wang, Y.; Tu, W.; Hong, J.; Zhang, W.; Xu, R. Molybdenum carbide microcrystals: Efficient and stable catalyst for photocatalytic H_2 evolution from water in the presence of dye sensitizer. *J. Mater.* **2016**, *2*, 344–349. [CrossRef]
210. Zhang, H.; Xin, C.; Wang, X.; Wang, K. Facile synthesis of Cd0.2Zn0.8 S-ethylenediamine hybrid solid solution and its improved photocatalytic performance. *Int. J. Hydrogen Energy* **2016**, *41*, 12019–12028. [CrossRef]
211. Wen, J.; Xie, J.; Shen, R.; Li, X.; Luo, X.; Zhang, H.; Zhang, A.; Bi, G. Markedly enhanced visible-light photocatalytic H_2 generation over gC_3N_4 nanosheets decorated by robust nickel phosphide ($Ni_{12}P_5$) cocatalysts. *Dalton Trans.* **2017**, *46*, 1794–1802. [CrossRef]
212. Wu, W.; Zhang, J.; Fan, W.; Li, Z.; Wang, L.; Li, X.; Wang, Y.; Wang, R.; Zheng, J.; Wu, M. Remedying defects in carbon nitride to improve both photooxidation and H_2 generation efficiencies. *ACS Catal.* **2016**, *6*, 3365–3371. [CrossRef]
213. Xie, L.; Ai, Z.; Zhang, M.; Sun, R.; Zhao, W. Enhanced Hydrogen Evolution in the Presence of Plasmonic Au-Photo-Sensitized g-C_3N_4 with an Extended Absorption Spectrum from 460 to 640 nm. *PLoS ONE* **2016**, *11*, e0161397. [CrossRef]
214. Xing, W.; Chen, G.; Li, C.; Sun, J.; Han, Z.; Zhou, Y.; Hu, Y.; Meng, Q. Construction of Large-Scale Ultrathin Graphitic Carbon Nitride Nanosheets by a Hydrogen-Bond-Assisted Strategy for Improved Photocatalytic Hydrogen Production and Ciprofloxacin Degradation Activity. *ChemCatChem* **2016**, *8*, 2838–2845. [CrossRef]

215. Feng, W.; Zhang, L.; Zhang, Y.; Yang, Y.; Fang, Z.; Wang, B.; Zhang, S.; Liu, P. Near-infrared-activated $NaYF_4$:Yb^{3+}, Er^{3+}/Au/CdS for H_2 production via photoreforming of bio-ethanol: Plasmonic Au as light nanoantenna, energy relay, electron sink and co-catalyst. *J. Mater. Chem. A* **2017**, *5*, 10311–10320. [CrossRef]
216. Yan, M.; Hua, Y.; Zhu, F.; Sun, L.; Gu, W.; Shi, W. Constructing nitrogen doped graphene quantum dots-ZnNb 2 O 6/gC_3N_4 catalysts for hydrogen production under visible light. *Appl. Catal. B Environ.* **2017**, *206*, 531–537. [CrossRef]
217. Yang, C.; Zhang, X.; Qin, J.; Shen, X.; Yu, R.; Ma, M.; Liu, R. Porous carbon-doped TiO_2 on TiC nanostructures for enhanced photocatalytic hydrogen production under visible light. *J. Catal.* **2017**, *347*, 36–44. [CrossRef]
218. Yang, L.; Huang, J.; Shi, L.; Cao, L.; Yu, Q.; Jie, Y.; Fei, J.; Ouyang, H.; Ye, J. A surface modification resultant thermally oxidized porous g-C_3N_4 with enhanced photocatalytic hydrogen production. *Appl. Catal. B Environ.* **2017**, *204*, 335–345. [CrossRef]
219. Ye, P.; Liu, X.; Iocozzia, J.; Yuan, Y.; Gu, L.; Xu, G.; Lin, Z. A highly stable non-noble metal Ni_2P co-catalyst for increased H_2 generation by gC_3N_4 under visible light irradiation. *J. Mater. Chem. A* **2017**, *5*, 8493–8498. [CrossRef]
220. Di, T.; Zhu, B.; Zhang, J.; Cheng, B.; Yu, J. Enhanced photocatalytic H_2 production on CdS nanorod using cobalt-phosphate as oxidation cocatalyst. *Appl. Surf. Sci.* **2016**, *389*, 775–782. [CrossRef]
221. Yue, X.; Yi, S.; Wang, R.; Zhang, Z.; Qiu, S. A novel architecture of dandelion-like Mo_2C/TiO_2 heterojunction photocatalysts towards high-performance photocatalytic hydrogen production from water splitting. *J. Mater. Chem. A* **2017**, *5*, 10591–10598. [CrossRef]
222. Zeng, Y.; Wang, Y.; Chen, J.; Jiang, Y.; Kiani, M.; Li, B.; Wang, R. Fabrication of high-activity hybrid $NiTiO_3$/gC_3N_4 heterostructured photocatalysts for water splitting to enhanced hydrogen production. *Ceram. Int.* **2016**, *42*, 12297–12305. [CrossRef]
223. Zeng, Z.; Li, K.; Wei, K.; Dai, Y.; Yan, L.; Guo, H.; Luo, X. Fabrication of porous gC_3N_4 and supported porous gC_3N_4 by a simple precursor pretreatment strategy and their efficient visible-light photocatalytic activity. *Chin. J. Catal.* **2017**, *38*, 498–507. [CrossRef]
224. Zha, D.-W.; Li, L.-F.; Pan, Y.-X.; He, J.-B. Coconut shell carbon nanosheets facilitating electron transfer for highly efficient visible-light-driven photocatalytic hydrogen production from water. *Int. J. Hydrogen Energy* **2016**, *41*, 17370–17379. [CrossRef]
225. Ge, M.; Li, Q.; Cao, C.; Huang, J.; Li, S.; Zhang, S.; Chen, Z.; Zhang, K.; Al-Deyab, S.S.; Lai, Y. One-dimensional TiO_2 Nanotube Photocatalysts for Solar Water Splitting. *Adv. Sci.* **2017**, *4*, 1600152. [CrossRef]
226. Zhang, P.; Song, T.; Wang, T.; Zeng, H. In-situ synthesis of Cu nanoparticles hybridized with carbon quantum dots as a broad spectrum photocatalyst for improvement of photocatalytic H_2 evolution. *Appl. Catal. B Environ.* **2017**, *206*, 328–335. [CrossRef]
227. Zhou, X.; Sun, H.; Zhang, H.; Tu, W. One-pot hydrothermal synthesis of CdS/NiS photocatalysts for high H_2 evolution from water under visible light. *Int. J. Hydrogen Energy* **2017**, *42*, 11199–11205. [CrossRef]
228. Zhao, W.; Xie, L.; Zhang, M.; Ai, Z.; Xi, H.; Li, Y.; Shi, Q.; Chen, J. Enhanced photocatalytic activity of all-solid-state gC_3N_4/Au/P_{25} Z-scheme system for visible-light-driven H_2 evolution. *Int. J. Hydrogen Energy* **2016**, *41*, 6277–6287. [CrossRef]
229. Zou, J.-P.; Wang, L.-C.; Luo, J.; Nie, Y.-C.; Xing, Q.-J.; Luo, X.-B.; Du, H.-M.; Luo, S.-L.; Suib, S.L. Synthesis and efficient visible light photocatalytic H_2 evolution of a metal-free gC_3N_4/graphene quantum dots hybrid photocatalyst. *Appl. Catal. B Environ.* **2016**, *193*, 103–109. [CrossRef]
230. Chu, J.; Han, X.; Yu, Z.; Du, Y.; Song, B.; Xu, P. Highly Efficient Visible-Light-Driven Photocatalytic Hydrogen Production on CdS/Cu_7S_4/g-C_3N_4 Ternary Heterostructures. *ACS Appl. Mater. Interfaces* **2018**, *10*, 20404–20411. [CrossRef]
231. Hua, S.; Qu, D.; An, L.; Jiang, W.; Wen, Y.; Wang, X.; Sun, Z. Highly efficient p-type Cu_3P/n-type g-C_3N_4 photocatalyst through Z-scheme charge transfer route. *Appl. Catal. B Environ.* **2019**, *240*, 253–261. [CrossRef]
232. Wang, P.; Guan, Z.; Li, Q.; Yang, J. Efficient visible-light-driven photocatalytic hydrogen production from water by using Eosin Y-sensitized novel g-C_3N_4/Pt/GO composites. *J. Mater. Sci.* **2018**, *53*, 774–786. [CrossRef]
233. Liu, J.; Jia, Q.; Long, J.; Wang, X.; Gao, Z.; Gu, Q. Amorphous NiO as co-catalyst for enhanced visible-light-driven hydrogen generation over g-C_3N_4 photocatalyst. *Appl. Catal. B Environ.* **2018**, *222*, 35–43. [CrossRef]

234. Fu, J.; Xu, Q.; Low, J.; Jiang, C.; Yu, J. Ultrathin 2D/2D WO_3/g-C_3N_4 step-scheme H_2-production photocatalyst. *Appl. Catal. B Environ.* **2019**, *243*, 556–565. [CrossRef]
235. de Castro, S.; da Silva, A.F.; Felix, J.F.; Piton, M.R.; Galeti, H.V.A.; Rodrigues, A.D.G.; Gobato, Y.G.; Al Saqri, N.; Henini, M.; Albadri, A.M.; et al. Effect of growth techniques on the structural, optical and electrical properties of indium doped TiO_2 thin films. *J. Alloys Compd.* **2018**, *766*, 194–203.
236. Yu, Y.; Yan, W.; Wang, X.; Li, P.; Gao, W.; Zou, H.; Wu, S.; Ding, K. Surface Engineering for Extremely Enhanced Charge Separation and Photocatalytic Hydrogen Evolution on g-C_3N_4. *Adv. Mater.* **2018**, *30*, 1705060. [CrossRef] [PubMed]
237. Ma, B.; Li, D.; Wang, X.; Lin, K. Molybdenum-Based Co-catalysts in Photocatalytic Hydrogen Production: Categories, Structures, and Roles. *ChemSusChem* **2018**, *11*, 3871–3881. [CrossRef]
238. Acar, C.; Dincer, I.; Naterer, G.F. Review of photocatalytic water-splitting methods for sustainable hydrogen production. *Int. J. Energy Res.* **2016**, *40*, 1449–1473. [CrossRef]
239. Alkaim, A.F.; Kandiel, T.A.; Dillert, R.; Bahnemann, D.W. Photocatalytic hydrogen production from biomass-derived compounds: A case study of citric acid. *Environ. Technol.* **2016**, *37*, 2687–2693. [CrossRef]
240. Almahdi, M.; Dincer, I.; Rosen, M. Analysis and assessment of methanol production by integration of carbon capture and photocatalytic hydrogen production. *Int. J. Greenh. Gas Control* **2016**, *51*, 56–70. [CrossRef]
241. Cai, Q.; Hu, Z.; Zhang, Q.; Li, B.; Shen, Z. Fullerene (C_{60})/CdS nanocomposite with enhanced photocatalytic activity and stability. *Appl. Surf. Sci.* **2017**, *403*, 151–158. [CrossRef]
242. Cai, X.; Li, G.; Yang, Y.; Zhang, C.; Yang, X. Cobalt thiolate complexes catalyst in noble-metal-free system for photocatalytic hydrogen production. *Russ. J. Appl. Chem.* **2016**, *89*, 1506–1511. [CrossRef]
243. Chang, C.-J.; Chu, K.-W. ZnS/polyaniline composites with improved dispersing stability and high photocatalytic hydrogen production activity. *Int. J. Hydrogen Energy* **2016**, *41*, 21764–21773. [CrossRef]
244. Chang, C.-J.; Lee, Z.; Chu, K.-W.; Wei, Y.-H. $CoFe_2O_4$@ ZnS core–shell spheres as magnetically recyclable photocatalysts for hydrogen production. *J. Taiwan Ins. Chem. Eng.* **2016**, *66*, 386–393. [CrossRef]
245. Chang, K.; Hai, X.; Ye, J. Transition Metal Disulfides as Noble-Metal-Alternative Co-Catalysts for Solar Hydrogen Production. *Adv. Energy Mater.* **2016**, *6*, 1502555. [CrossRef]
246. Chen, H.; Jiang, D.; Sun, Z.; Irfan, R.M.; Zhang, L.; Du, P. Cobalt nitride as an efficient cocatalyst on CdS nanorods for enhanced photocatalytic hydrogen production in water. *Catal. Sci. Technol.* **2017**, *7*, 1515–1522. [CrossRef]
247. Chen, T.; Song, C.; Fan, M.; Hong, Y.; Hu, B.; Yu, L.; Shi, W. In-situ fabrication of CuS/gC_3N_4 nanocomposites with enhanced photocatalytic H_2-production activity via photoinduced interfacial charge transfer. *Int. J. Hydrogen Energy* **2017**, *42*, 12210–12219. [CrossRef]
248. Chen, Y.; Tian, G.; Zhou, W.; Xiao, Y.; Wang, J.; Zhang, X.; Fu, H. Enhanced photogenerated carrier separation in CdS quantum dot sensitized $ZnFe_2O_4$/$ZnIn_2S_4$ nanosheet stereoscopic films for exceptional visible light photocatalytic H_2 evolution performance. *Nanoscale* **2017**, *9*, 5912–5921. [CrossRef]
249. Chu, J.; Han, X.; Yu, Z.; Du, Y.; Song, B.; Xu, P. Fabrication of H-TiO_2/CdS/Cu_2-xS Ternary Heterostructures for Enhanced Photocatalytic Hydrogen Production. *ChemistrySelect* **2017**, *2*, 2684–2689. [CrossRef]
250. Dong, M.; Zhou, P.; Jiang, C.; Cheng, B.; Yu, J. First-principles investigation of Cu-doped ZnS with enhanced photocatalytic hydrogen production activity. *Chem. Phys. Lett.* **2017**, *668*, 1–6. [CrossRef]
251. Du, R.; Zhang, Y.; Li, B.; Yu, X.; Liu, H.; An, X.; Qu, J. Biomolecule-assisted synthesis of defect-mediated $Cd_{1-x}Zn_xS$/MoS_2/graphene hollow spheres for highly efficient hydrogen evolution. *Phys. Chem. Chem. Phys.* **2016**, *18*, 16208–16215. [CrossRef]
252. Fang, X.; Song, J.; Shi, H.; Kang, S.; Li, Y.; Sun, G.; Cui, L. Enhanced efficiency and stability of $Co_{0.5}Cd_{0.5}S$/gC_3N_4 composite photo-catalysts for hydrogen evolution from water under visible light irradiation. *Int. J. Hydrogen Energy* **2017**, *42*, 5741–5748. [CrossRef]
253. Feng, W.; Fang, Z.; Wang, B.; Zhang, L.; Zhang, Y.; Yang, Y.; Huang, M.; Weng, S.; Liu, P. Grain boundary engineering in organic–inorganic hybrid semiconductor ZnS (en) 0.5 for visible-light photocatalytic hydrogen production. *J. Mater. Chem. A* **2017**, *5*, 1387–1393. [CrossRef]
254. García-Mendoza, C.; Oros-Ruiz, S.; Hernández-Gordillo, A.; López, R.; Jácome-Acatitla, G.; Calderón, H.A.; Gómez, R. Suitable preparation of Bi_2S_3 nanorods–TiO_2 heterojunction semiconductors with improved photocatalytic hydrogen production from water/methanol decomposition. *J. Chem. Technol. Biotechnol.* **2016**, *91*, 2198–2204. [CrossRef]

255. Gu, Q.; Sun, H.; Xie, Z.; Gao, Z.; Xue, C. MoS_2-coated microspheres of self-sensitized carbon nitride for efficient photocatalytic hydrogen generation under visible light irradiation. *Appl. Surf. Sci.* **2017**, *396*, 1808–1815. [CrossRef]
256. Guo, H.-L.; Du, H.; Jiang, Y.-F.; Jiang, N.; Shen, C.-C.; Zhou, X.; Liu, Y.-N.; Xu, A.-W. Artificial Photosynthetic Z-scheme Photocatalyst for Hydrogen Evolution with High Quantum Efficiency. *J. Phys. Chem. C* **2016**, *121*, 107–114. [CrossRef]
257. Guo, X.; Chen, Y.; Qin, Z.; Wang, M.; Guo, L. One-step hydrothermal synthesis of $Zn_xCd_{1-x}S$/ZnO heterostructures for efficient photocatalytic hydrogen production. *Int. J. Hydrogen Energy* **2016**, *41*, 15208–15217. [CrossRef]
258. Ha, E.; Liu, W.; Wang, L.; Man, H.-W.; Hu, L.; Tsang, S.C.E.; Chan, C.T.-L.; Kwok, W.-M.; Lee, L.Y.S.; Wong, K.-Y. Cu_2ZnSnS_4/MoS_2-Reduced Graphene Oxide Heterostructure: Nanoscale Interfacial Contact and Enhanced Photocatalytic Hydrogen Generation. *Sci. Rep.* **2017**, *7*, 39411. [CrossRef]
259. Hai, X.; Zhou, W.; Chang, K.; Pang, H.; Liu, H.; Shi, L.; Ichihara, F.; Ye, J. Engineering the crystallinity of MoS 2 monolayers for highly efficient solar hydrogen production. *J. Mater. Chem. A* **2017**, *5*, 8591–8598. [CrossRef]
260. Hong, S.; Kumar, D.P.; Reddy, D.A.; Choi, J.; Kim, T.K. Excellent photocatalytic hydrogen production over CdS nanorods via using noble metal-free copper molybdenum sulfide (Cu_2MoS_4) nanosheets as co-catalysts. *Appl. Surf. Sci.* **2017**, *396*, 421–429. [CrossRef]
261. Hu, P.; Ngaw, C.K.; Yuan, Y.; Bassi, P.S.; Loo, S.C.J.; Tan, T.T.Y. Bandgap engineering of ternary sulfide nanocrystals by solution proton alloying for efficient photocatalytic H_2 evolution. *Nano Energy* **2016**, *26*, 577–585. [CrossRef]
262. Hu, S.; Zhu, M. Enhanced Solar Hydrogen Generation by a Heterojunction of Perovskite-type $La_2Ti_2O_7$ Nanosheets Doped with CdS Quantum Dots. *ChemPlusChem* **2016**, *81*, 1202–1208. [CrossRef]
263. Huang, E.; Yao, X.; Wang, W.; Wu, G.; Guan, N.; Li, L. SnS_2 Nanoplates with Specific Facets Exposed for Enhanced Visible-Light-Driven Photocatalysis. *ChemPhotoChem* **2017**, *1*, 60–69. [CrossRef]
264. Huang, H.; Dai, B.; Wang, W.; Lu, C.; Kou, J.; Ni, Y.; Wang, L.; Xu, Z. Oriented Built-in Electric Field Introduced by Surface Gradient Diffusion Doping for Enhanced Photocatalytic H_2 Evolution in CdS Nanorods. *Nano Lett.* **2017**, *17*, 3803–3808. [CrossRef]
265. Huang, T.; Chen, W.; Liu, T.-Y.; Hao, Q.-L.; Liu, X.-H. Hybrid of AgInZnS and MoS_2 as efficient visible-light driven photocatalyst for hydrogen production. *Int. J. Hydrogen Energy* **2017**, *42*, 12254–12261. [CrossRef]
266. Huang, T.; Chen, W.; Liu, T.-Y.; Hao, Q.-L.; Liu, X.-H. $ZnIn_2S_4$ hybrid with MoS_2: A non-noble metal photocatalyst with efficient photocatalytic activity for hydrogen evolution. *Powder Technol.* **2017**, *315*, 157–162. [CrossRef]
267. Irfan, R.M.; Jiang, D.; Sun, Z.; Lu, D.; Du, P. Enhanced photocatalytic H_2 production on CdS nanorods with simple molecular bidentate cobalt complexes as cocatalysts under visible light. *Dalton Trans.* **2016**, *45*, 12897–12905. [CrossRef]
268. Jiang, F.; Pan, B.; You, D.; Zhou, Y.; Wang, X.; Su, W. Visible light photocatalytic H_2-production activity of epitaxial Cu_2ZnSnS_4/ZnS heterojunction. *Catal. Commun.* **2016**, *85*, 39–43. [CrossRef]
269. Jiang, Z.; Liu, J.; Gao, M.; Fan, X.; Zhang, L.; Zhang, J. Assembling Polyoxo-Titanium Clusters and CdS Nanoparticles to a Porous Matrix for Efficient and Tunable H_2-Evolution Activities with Visible Light. *Adv. Mater.* **2017**, *29*, 1603369. [CrossRef]
270. Jo, W.-K.; Selvam, N.C.S. Fabrication of photostable ternary CdS/MoS_2/MWCNTs hybrid photocatalysts with enhanced H_2 generation activity. *Appl. Catal. A Gen.* **2016**, *525*, 9–22. [CrossRef]
271. Kandiel, T.A.; Takanabe, K. Solvent-induced deposition of Cu–Ga–In–S nanocrystals onto a titanium dioxide surface for visible-light-driven photocatalytic hydrogen production. *Appl. Catal. B Environ.* **2016**, *184*, 264–269. [CrossRef]
272. Kaur, M.; Nagaraja, C. Template-Free Synthesis of $Zn_{1-x}Cd_xS$ Nanocrystals with Tunable Band Structure for Efficient Water Splitting and Reduction of Nitroaromatics in Water. *ACS Sustain. Chem. Eng.* **2017**, *5*, 4293–4303. [CrossRef]
273. Kim, Y.G.; Jo, W.-K. Photodeposited-metal/CdS/ZnO heterostructures for solar photocatalytic hydrogen production under different conditions. *Int. J. Hydrogen Energy* **2017**, *42*, 11356–11363. [CrossRef]
274. Kim, Y.K.; Lim, S.K.; Park, H.; Hoffmann, M.R.; Kim, S. Trilayer CdS/carbon nanofiber (CNF) mat/Pt-TiO_2 composite structures for solar hydrogen production: Effects of CNF mat thickness. *Appl. Catal. B Environ.* **2016**, *196*, 216–222. [CrossRef]

275. Kimi, M.; Yuliati, L.; Shamsuddin, M. Preparation and characterization of In and Cu co-doped ZnS photocatalysts for hydrogen production under visible light irradiation. *J. Energy Chem.* **2016**, *25*, 512–516. [CrossRef]
276. Kong, Z.; Yuan, Y.-J.; Chen, D.; Fang, G.; Yang, Y.; Yang, S.; Cao, D. Noble-metal-free MoS_2 nanosheet modified-$InVO_4$ heterostructures for enhanced visible-light-driven photocatalytic H_2 production. *Dalton Trans.* **2017**, *46*, 2072–2076. [CrossRef] [PubMed]
277. Kumar, D.P.; Hong, S.; Reddy, D.A.; Kim, T.K. Ultrathin MoS_2 layers anchored exfoliated reduced graphene oxide nanosheet hybrid as a highly efficient cocatalyst for CdS nanorods towards enhanced photocatalytic hydrogen production. *Appl. Catal. B Environ.* **2017**, *212*, 7–14. [CrossRef]
278. Leo, I.M.; Soto, E.; Vaquero, F.; Mota, N.; Navarro, R.; Fierro, J. Influence of the reduction of graphene oxide (rGO) on the structure and photoactivity of CdS-rGO hybrid systems. *Int. J. Hydrogen Energy* **2017**, *42*, 13691–13703.
279. Li, M.; Zhang, L.; Fan, X.; Wu, M.; Du, Y.; Wang, M.; Kong, Q.; Zhang, L.; Shi, J. Dual synergetic effects in MoS_2/pyridine-modified gC_3N_4 composite for highly active and stable photocatalytic hydrogen evolution under visible light. *Appl. Catal. B Environ.* **2016**, *190*, 36–43. [CrossRef]
280. Li, X.; Liu, H.; Liu, S.; Zhang, J.; Chen, W.; Huang, C.; Mao, L. Effect of Pt–Pd hybrid nano-particle on CdS's activity for water splitting under visible light. *Int. J. Hydrogen Energy* **2016**, *41*, 23015–23021. [CrossRef]
281. Li, Y.; Hou, Y.; Fu, Q.; Peng, S.; Hu, Y.H. Oriented growth of $ZnIn_2S_4$/$In(OH)_3$ heterojunction by a facile hydrothermal transformation for efficient photocatalytic H_2 production. *Appl. Catal. B Environ.* **2017**, *206*, 726–733. [CrossRef]
282. Li, Y.; Jin, R.; Xing, Y.; Li, J.; Song, S.; Liu, X.; Li, M.; Jin, R. Macroscopic Foam-Like Holey Ultrathin g-C_3N_4 Nanosheets for Drastic Improvement of Visible-Light Photocatalytic Activity. *Adv. Energy Mater.* **2016**, *6*, 1601273. [CrossRef]
283. Li, Z.; Chen, X.; Shangguan, W.; Su, Y.; Liu, Y.; Dong, X.; Sharma, P.; Zhang, Y. Prickly Ni_3S_2 nanowires modified CdS nanoparticles for highly enhanced visible-light photocatalytic H_2 production. *Int. J. Hydrogen Energy* **2017**, *42*, 6618–6626. [CrossRef]
284. Lin, H.; Li, Y.; Li, H.; Wang, X. Multi-node CdS hetero-nanowires grown with defect-rich oxygen-doped MoS_2 ultrathin nanosheets for efficient visible-light photocatalytic H_2 evolution. *Nano Res.* **2017**, *10*, 1377–1392. [CrossRef]
285. Liu, H.; Xu, Z.; Zhang, Z.; Ao, D. Novel visible-light driven $Mn_{0.8}Cd_{0.2}S$/gC_3N_4 composites: Preparation and efficient photocatalytic hydrogen production from water without noble metals. *Appl. Catal. A Gen.* **2016**, *518*, 150–157. [CrossRef]
286. Liu, M.; Chen, Y.; Su, J.; Shi, J.; Wang, X.; Guo, L. Photocatalytic hydrogen production using twinned nanocrystals and an unanchored NiSx co-catalyst. *Nat. Energy* **2016**, *1*, 16151. [CrossRef]
287. Liu, X.; Xing, Z.; Zhang, Y.; Li, Z.; Wu, X.; Tan, S.; Yu, X.; Zhu, Q.; Zhou, W. Fabrication of 3D flower-like black N-TiO_2-x@ MoS_2 for unprecedented-high visible-light-driven photocatalytic performance. *Appl. Catal. B Environ.* **2017**, *201*, 119–127. [CrossRef]
288. Liu, Y.; Tang, C. Enhancement of photocatalytic H_2 evolution over TiO_2 nano-sheet films by surface loading NiS nanoparticles. *Russ. J. Phys. Chem. A* **2016**, *90*, 1042–1048. [CrossRef]
289. Lu, D.; Wang, H.; Zhao, X.; Kondamareddy, K.K.; Ding, J.; Li, C.; Fang, P. Highly efficient visible-light-induced photoactivity of Z-scheme g-C_3N_4/Ag/MoS_2 ternary photocatalysts for organic pollutant degradation and production of hydrogen. *ACS Sustain. Chem. Eng.* **2017**, *5*, 1436–1445. [CrossRef]
290. Ma, L.; Chen, K.; Nan, F.; Wang, J.H.; Yang, D.J.; Zhou, L.; Wang, Q.Q. Improved Hydrogen Production of Au–Pt–CdS Hetero-Nanostructures by Efficient Plasmon-Induced Multipathway Electron Transfer. *Adv. Funct. Mater.* **2016**, *26*, 6076–6083. [CrossRef]
291. Ma, X.; Li, J.; An, C.; Feng, J.; Chi, Y.; Liu, J.; Zhang, J.; Sun, Y. Ultrathin Co (Ni)-doped MoS- nanosheets as catalytic promoters enabling efficient solar hydrogen production. *Nano Res.* **2016**, *9*, 2284–2293. [CrossRef]
292. Majeed, I.; Nadeem, M.A.; Hussain, E.; Badshah, A.; Gilani, R.; Nadeem, M.A. Effect of deposition method on metal loading and photocatalytic activity of Au/CdS for hydrogen production in water electrolyte mixture. *Int. J. Hydrogen Energy* **2017**, *42*, 3006–3018. [CrossRef]
293. Malekshoar, G.; Ray, A.K. In-situ grown molybdenum sulfide on TiO_2 for dye-sensitized solar photocatalytic hydrogen generation. *Chem. Eng. Sci.* **2016**, *152*, 35–44. [CrossRef]

294. Mancipe, S.; Tzompantzi, F.; Gómez, R. Synthesis of CdS/MgAl layered double hydroxides for hydrogen production from methanol-water decomposition. *Appl. Clay Sci.* **2017**, *136*, 67–74. [CrossRef]
295. Manjunath, K.; Souza, V.; Nagaraju, G.; Santos, J.M.L.; Dupont, J.; Ramakrishnappa, T. Superior activity of the CuS–TiO_2/Pt hybrid nanostructure towards visible light induced hydrogen production. *New J. Chem.* **2016**, *40*, 10172–10180. [CrossRef]
296. Mei, Z.; Zhang, M.; Schneider, J.; Wang, W.; Zhang, N.; Su, Y.; Chen, B.; Wang, S.; Rogach, A.L.; Pan, F. Hexagonal $Zn_{1-x}Cd_xS$ ($0.2 \leq x \leq 1$) solid solution photocatalysts for H_2 generation from water. *Catal. Sci. Technol.* **2017**, *7*, 982–987. [CrossRef]
297. Nandy, S.; Goto, Y.; Hisatomi, T.; Moriya, Y.; Minegishi, T.; Katayama, M.; Domen, K. Synthesis and Photocatalytic Activity of La_5Ti_2Cu $(S_{1-x}Se_x)_5O_7$ Solid Solutions for H_2 Production under Visible Light Irradiation. *ChemPhotoChem* **2017**, *1*, 265–272. [CrossRef]
298. Núñez, J.; Fresno, F.; Collado, L.; Jana, P.; Coronado, J.M.; Serrano, D.P.; Víctor, A. Photocatalytic H_2 production from aqueous methanol solutions using metal-co-catalysed Zn_2SnO_4 nanostructures. *Appl. Catal. B Environ.* **2016**, *191*, 106–115. [CrossRef]
299. Oros-Ruiz, S.; Hernández-Gordillo, A.; García-Mendoza, C.; Rodríguez-Rodríguez, A.A.; Gomez, R. Comparative activity of CdS nanofibers superficially modified by Au, Cu, and Ni nanoparticles as co-catalysts for photocatalytic hydrogen production under visible light. *J. Chem. Technol. Biotechnol.* **2016**, *91*, 2205–2210. [CrossRef]
300. Park, H.; Ou, H.-H.; Kim, M.; Kang, U.; Han, D.S.; Hoffmann, M.R. Photocatalytic H_2 production on trititanate nanotubes coupled with CdS and platinum nanoparticles under visible light: Revisiting H_2 production and material durability. *Faraday Discuss.* **2017**, *198*, 419–431. [CrossRef]
301. Qiu, F.; Han, Z.; Peterson, J.J.; Odoi, M.Y.; Sowers, K.L.; Krauss, T.D. Photocatalytic hydrogen generation by CdSe/CdS nanoparticles. *Nano Lett.* **2016**, *16*, 5347–5352. [CrossRef] [PubMed]
302. Rahman, M.; Davey, K.; Qiao, S.Z. Counteracting Blueshift Optical Absorption and Maximizing Photon Harvest in Carbon Nitride Nanosheets Photocatalyst. *Small* **2017**, *13*, 1700376. [CrossRef]
303. Rahmawati, F.; Yuliati, L.; Alaih, I.S.; Putri, F.R. Carbon rod of zinc-carbon primary battery waste as a substrate for CdS and TiO_2 photocatalyst layer for visible light driven photocatalytic hydrogen production. *J. Environ. Chem. Eng.* **2017**, *5*, 2251–2258. [CrossRef]
304. Ran, J.; Gao, G.; Li, F.-T.; Ma, T.-Y.; Du, A.; Qiao, S.-Z. Ti_3C_2 MXene co-catalyst on metal sulfide photo-absorbers for enhanced visible-light photocatalytic hydrogen production. *Nat. Commun.* **2017**, *8*, 13907. [CrossRef]
305. Rao, H.; Yu, W.-Q.; Zheng, H.-Q.; Bonin, J.; Fan, Y.-T.; Hou, H.-W. Highly efficient photocatalytic hydrogen evolution from nickel quinolinethiolate complexes under visible light irradiation. *J. Power Sources* **2016**, *324*, 253–260. [CrossRef]
306. Reddy, D.A.; Park, H.; Hong, S.; Kumar, D.P.; Kim, T.K. Hydrazine-assisted formation of ultrathin MoS_2 nanosheets for enhancing their co-catalytic activity in photocatalytic hydrogen evolution. *J. Mater. Chem. A* **2017**, *5*, 6981–6991. [CrossRef]
307. Reddy, D.A.; Park, H.; Ma, R.; Kumar, D.P.; Lim, M.; Kim, T.K. Heterostructured WS_2-MoS_2 Ultrathin Nanosheets Integrated on CdS Nanorods to Promote Charge Separation and Migration and Improve Solar-Driven Photocatalytic Hydrogen Evolution. *ChemSusChem* **2017**, *10*, 1563–1570. [CrossRef] [PubMed]
308. Shi, Z.; Dong, X.; Dang, H. Facile fabrication of novel red phosphorus-CdS composite photocatalysts for H_2 evolution under visible light irradiation. *Int. J. Hydrogen Energy* **2016**, *41*, 5908–5915. [CrossRef]
309. Sola, A.; Homs, N.; de la Piscina, P.R. Photocatalytic H_2 production from ethanol (aq) solutions: The effect of intermediate products. *Int. J. Hydrogen Energy* **2016**, *41*, 19629–19636. [CrossRef]
310. Souza, E.A.; Silva, L.A. Energy recovery from tannery sludge wastewaters through photocatalytic hydrogen production. *J. Environ. Chem. Eng.* **2016**, *4*, 2114–2120. [CrossRef]
311. Su, J.; Zhang, T.; Li, Y.; Chen, Y.; Liu, M. Photocatalytic activities of copper doped cadmium sulfide microspheres prepared by a facile ultrasonic spray-pyrolysis method. *Molecules* **2016**, *21*, 735. [CrossRef]
312. Vaquero, F.; Navarro, R.; Fierro, J. Evolution of the nanostructure of CdS using solvothermal synthesis at different temperature and its influence on the photoactivity for hydrogen production. *Int. J. Hydrogen Energy* **2016**, *41*, 11558–11567. [CrossRef]

313. Sun, S.; Gao, P.; Yang, Y.; Yang, P.; Chen, Y.; Wang, Y. N-doped TiO_2 nanobelts with coexposed (001) and (101) facets and their highly efficient visible-light-driven photocatalytic hydrogen production. *ACS Appl. Mater. Interfaces* **2016**, *8*, 18126–18131. [CrossRef]
314. Wang, F.; Jin, Z.; Jiang, Y.; Backus, E.H.; Bonn, M.; Lou, S.N.; Turchinovich, D.; Amal, R. Probing the charge separation process on In_2S_3/Pt-TiO_2 nanocomposites for boosted visible-light photocatalytic hydrogen production. *Appl. Catal. B Environ.* **2016**, *198*, 25–31. [CrossRef]
315. Wang, H.; Li, Y.; Shu, D.; Chen, X.; Liu, X.; Wang, X.; Zhang, J.; Wang, H. CoPtx-loaded $Zn_{0.5}Cd_{0.5}S$ nanocomposites for enhanced visible light photocatalytic H_2 production. *Int. J. Energy Res.* **2016**, *40*, 1280–1286. [CrossRef]
316. Wang, J.; Chen, Y.; Zhou, W.; Tian, G.; Xiao, Y.; Fu, H.; Fu, H. Cubic quantum dot/hexagonal microsphere $ZnIn_2S_4$ heterophase junctions for exceptional visible-light-driven photocatalytic H_2 evolution. *J. Mater. Chem. A* **2017**, *5*, 8451–8460. [CrossRef]
317. Wang, J.; Wang, Z.; Zhu, Z. Synergetic effect of $Ni(OH)_2$ cocatalyst and CNT for high hydrogen generation on CdS quantum dot sensitized TiO_2 photocatalyst. *Appl. Catal. B Environ.* **2017**, *204*, 577–583. [CrossRef]
318. Wang, L.; Di, Q.; Sun, M.; Liu, J.; Cao, C.; Liu, J.; Xu, M.; Zhang, J. Assembly-promoted photocatalysis: Three-dimensional assembly of CdS_xSe_{1-x} (x = 0–1) quantum dots into nanospheres with enhanced photocatalytic performance. *J. Mater.* **2017**, *3*, 63–70. [CrossRef]
319. Wang, Y.; Zhang, Y.; Jiang, Z.; Jiang, G.; Zhao, Z.; Wu, Q.; Liu, Y.; Xu, Q.; Duan, A.; Xu, C. Controlled fabrication and enhanced visible-light photocatalytic hydrogen production of Au@ CdS/MIL-101 heterostructure. *Appl. Catal. B Environ.* **2016**, *185*, 307–314. [CrossRef]
320. Wang, Z.; Wang, S.; Liu, J.; Jiang, W.; Zhou, Y.; An, C.; Zhang, J. Synthesis of $AgInS_2$-xAg_2S-yZnS-zIn_6S_7 (x, y, z = 0, or 1) Nanocomposites with Composition-Dependent Activity towards Solar Hydrogen Evolution. *Materials* **2016**, *9*, 329. [CrossRef]
321. Wu, A.; Tian, C.; Jiao, Y.; Yan, Q.; Yang, G.; Fu, H. Sequential two-step hydrothermal growth of MoS_2/CdS core-shell heterojunctions for efficient visible light-driven photocatalytic H_2 evolution. *Appl. Catal. B Environ.* **2017**, *203*, 955–963. [CrossRef]
322. Wu, L.; Gong, J.; Ge, L.; Han, C.; Fang, S.; Xin, Y.; Li, Y.; Lu, Y. AuPd bimetallic nanoparticles decorated $Cd_{0.5}Zn_{0.5}S$ photocatalysts with enhanced visible-light photocatalytic H_2 production activity. *Int. J. Hydrogen Energy* **2016**, *41*, 14704–14712. [CrossRef]
323. Xia, Y.; Li, Q.; Lv, K.; Tang, D.; Li, M. Superiority of graphene over carbon analogs for enhanced photocatalytic H_2-production activity of $ZnIn_2S_4$. *Appl. Catal. B Environ.* **2017**, *206*, 344–352. [CrossRef]
324. Xin, Y.; Lu, Y.; Han, C.; Ge, L.; Qiu, P.; Li, Y.; Fang, S. Novel NiS cocatalyst decorating ultrathin 2D TiO_2 nanosheets with enhanced photocatalytic hydrogen evolution activity. *Mater. Res. Bull.* **2017**, *87*, 123–129. [CrossRef]
325. Xing, Z.; Zong, X.; Zhu, Y.; Chen, Z.; Bai, Y.; Wang, L. A nanohybrid of CdTe@ CdS nanocrystals and titania nanosheets with p–n nanojunctions for improved visible light-driven hydrogen production. *Catal. Today* **2016**, *264*, 229–235. [CrossRef]
326. Yan, J.; Li, X.; Yang, S.; Wang, X.; Zhou, W.; Fang, Y.; Zhang, S.; Peng, F.; Zhang, S. Design and preparation of CdS/H-3D-TiO_2/Pt-wire photocatalysis system with enhanced visible-light driven H_2 evolution. *Int. J. Hydrogen Energy* **2017**, *42*, 928–937. [CrossRef]
327. Yan, Q.; Wu, A.; Yan, H.; Dong, Y.; Tian, C.; Jiang, B.; Fu, H. Gelatin-assisted synthesis of ZnS hollow nanospheres: The microstructure tuning, formation mechanism and application for Pt-free photocatalytic hydrogen production. *CrystEngComm* **2017**, *19*, 461–468. [CrossRef]
328. Yang, L.; Guo, S.; Li, X. Au nanoparticles@ MoS_2 core-shell structures with moderate MoS_2 coverage for efficient photocatalytic water splitting. *J. Alloys Compd.* **2017**, *706*, 82–88. [CrossRef]
329. Yang, Y.; Zhang, Y.; Fang, Z.; Zhang, L.; Zheng, Z.; Wang, Z.; Feng, W.; Weng, S.; Zhang, S.; Liu, P. Simultaneous Realization of Enhanced Photoactivity and Promoted Photostability by Multilayered MoS_2 Coating on CdS Nanowire Structure via Compact Coating Methodology. *ACS Appl. Mater. Interfaces* **2017**, *9*, 6950–6958. [CrossRef]
330. Yu, X.; Shi, J.; Wang, L.; Wang, W.; Bian, J.; Feng, L.; Li, C. A novel Au NPs-loaded MoS_2/RGO composite for efficient hydrogen evolution under visible light. *Mater. Lett.* **2016**, *182*, 125–128. [CrossRef]

331. Yuan, Y.J.; Chen, D.Q.; Huang, Y.W.; Yu, Z.T.; Zhong, J.S.; Chen, T.T.; Tu, W.G.; Guan, Z.J.; Cao, D.P.; Zou, Z.G. MoS_2 Nanosheet-Modified $CuInS_2$ Photocatalyst for Visible-Light-Driven Hydrogen Production from Water. *ChemSusChem* **2016**, *9*, 1003–1009. [CrossRef]
332. Yuan, Y.-J.; Tu, J.-R.; Ye, Z.-J.; Chen, D.-Q.; Hu, B.; Huang, Y.-W.; Chen, T.-T.; Cao, D.-P.; Yu, Z.-T.; Zou, Z.-G. MoS_2-graphene/$ZnIn_2S_4$ hierarchical microarchitectures with an electron transport bridge between light-harvesting semiconductor and cocatalyst: A highly efficient photocatalyst for solar hydrogen generation. *Appl. Catal. B Environ.* **2016**, *188*, 13–22. [CrossRef]
333. Yue, Z.; Liu, A.; Zhang, C.; Huang, J.; Zhu, M.; Du, Y.; Yang, P. Noble-metal-free hetero-structural CdS/Nb_2O_5/N-doped-graphene ternary photocatalytic system as visible-light-driven photocatalyst for hydrogen evolution. *Appl. Catal. B Environ.* **2017**, *201*, 202–210. [CrossRef]
334. Zhang, J.; Yao, W.; Huang, C.; Shi, P.; Xu, Q. High efficiency and stable tungsten phosphide cocatalysts for photocatalytic hydrogen production. *J. Mater. Chem. A* **2017**, *5*, 12513–12519. [CrossRef]
335. Zhang, N.; Chen, D.; Cai, B.; Wang, S.; Niu, F.; Qin, L.; Huang, Y. Facile synthesis of CdS $ZnWO_4$ composite photocatalysts for efficient visible light driven hydrogen evolution. *Int. J. Hydrogen Energy* **2017**, *42*, 1962–1969. [CrossRef]
336. Zhang, S.; Wang, L.; Zeng, Y.; Xu, Y.; Tang, Y.; Luo, S.; Liu, Y.; Liu, C. CdS-Nanoparticles-Decorated Perpendicular Hybrid of MoS_2 and N-Doped Graphene Nanosheets for Omnidirectional Enhancement of Photocatalytic Hydrogen Evolution. *ChemCatChem* **2016**, *8*, 2557–2564. [CrossRef]
337. Zhang, Y.; Han, L.; Wang, C.; Wang, W.; Ling, T.; Yang, J.; Dong, C.; Lin, F.; Du, X.-W. Zinc-Blende CdS Nanocubes with Coordinated Facets for Photocatalytic Water Splitting. *ACS Catal.* **2017**, *7*, 1470–1477. [CrossRef]
338. Zhao, H.; Sun, R.; Li, X.; Sun, X. Enhanced photocatalytic activity for hydrogen evolution from water by $Zn_{0.5}Cd_{0.5}S/WS_2$ heterostructure. *Mater. Sci. Semicond. Process.* **2017**, *59*, 68–75. [CrossRef]
339. Zhou, X.; Huang, J.; Zhang, H.; Sun, H.; Tu, W. Controlled synthesis of CdS nanoparticles and their surface loading with MoS 2 for hydrogen evolution under visible light. *Int. J. Hydrogen Energy* **2016**, *41*, 14758–14767. [CrossRef]
340. Jiang, D.; Chen, X.; Zhang, Z.; Zhang, L.; Wang, Y.; Sun, Z.; Irfan, R.M.; Du, P. Highly efficient simultaneous hydrogen evolution and benzaldehyde production using cadmium sulfide nanorods decorated with small cobalt nanoparticles under visible light. *J. Catal.* **2018**, *357*, 147–153. [CrossRef]
341. Kumar, D.P.; Park, H.; Kim, E.H.; Hong, S.; Gopannagari, M.; Reddy, D.A.; Kim, T.K. Noble metal-free metal-organic framework-derived onion slice-type hollow cobalt sulfide nanostructures: Enhanced activity of CdS for improving photocatalytic hydrogen production. *Appl. Catal. B Environ.* **2018**, *224*, 230–238. [CrossRef]
342. Lv, J.-X.; Zhang, Z.-M.; Wang, J.; Lu, X.-L.; Zhang, W.; Lu, T.-B. In situ synthesis of CdS/graphdiyne heterojunction for enhanced photocatalytic activity of hydrogen production. *ACS Appl. Mater. Interfaces* **2019**, *11*, 2655–2661. [CrossRef]
343. Feng, C.; Chen, Z.; Hou, J.; Li, J.; Li, X.; Xu, L.; Sun, M.; Zeng, R. Effectively enhanced photocatalytic hydrogen production performance of one-pot synthesized MoS_2 clusters/CdS nanorod heterojunction material under visible light. *Chem. Eng. J.* **2018**, *345*, 404–413. [CrossRef]
344. Liu, Y.; Ma, Y.; Liu, W.; Shang, Y.; Zhu, A.; Tan, P.; Xiong, X.; Pan, J. Facet and morphology dependent photocatalytic hydrogen evolution with CdS nanoflowers using a novel mixed solvothermal strategy. *J. Colloid Interface Sci.* **2018**, *513*, 222–230. [CrossRef]
345. Wang, L.; Xu, N.; Pan, X.; He, Y.; Wang, X.; Su, W. Cobalt lactate complex as a hole cocatalyst for significantly enhanced photocatalytic H_2 production activity over CdS nanorods. *Catal. Sci. Technol.* **2018**, *8*, 1599–1605. [CrossRef]
346. Abe, R. Recent progress on photocatalytic and photoelectrochemical water splitting under visible light irradiation. *J. Photochem. Photobiol. C Photochem. Rev.* **2010**, *11*, 179–209. [CrossRef]
347. Ahmed, A.Y.; Kandiel, T.A.; Ivanova, I.; Bahnemann, D. Photocatalytic and photoelectrochemical oxidation mechanisms of methanol on TiO_2 in aqueous solution. *Appl. Surf. Sci.* **2014**, *319*, 44–49. [CrossRef]
348. Al-Ahmed, A.; Mukhtar, B.; Hossain, S.; Javaid Zaidi, S.; Rahman, S. Application of Titanium dioxide (TiO_2) based photocatalytic nanomaterials in Solar and Hydrogen Energy: A Short Review. *Mater. Sci. Forum* **2012**, *712*, 25–47. [CrossRef]

349. Amao, Y. Solar fuel production based on the artificial photosynthesis system. *ChemCatChem* **2011**, *3*, 458–474. [CrossRef]
350. An, X.; Jimmy, C.Y. Graphene-based photocatalytic composites. *RSC Adv.* **2011**, *1*, 1426–1434. [CrossRef]
351. Ashokkumar, M. An overview on semiconductor particulate systems for photoproduction of hydrogen. *Int. J. Hydrogen Energy* **1998**, *23*, 427–438. [CrossRef]
352. Babu, V.J.; Vempati, S.; Uyar, T.; Ramakrishna, S. Review of one-dimensional and two-dimensional nanostructured materials for hydrogen generation. *Phys. Chem. Chem. Phys.* **2015**, *17*, 2960–2986. [CrossRef]
353. Bai, S.; Yin, W.; Wang, L.; Li, Z.; Xiong, Y. Surface and interface design in cocatalysts for photocatalytic water splitting and CO_2 reduction. *RSC Adv.* **2016**, *6*, 57446–57463. [CrossRef]
354. Bowker, M. Sustainable hydrogen production by the application of ambient temperature photocatalysis. *Green Chem.* **2011**, *13*, 2235–2246. [CrossRef]
355. Chen, X.; Li, C.; Grätzel, M.; Kostecki, R.; Mao, S.S. Nanomaterials for renewable energy production and storage. *Chem. Soc. Rev.* **2012**, *41*, 7909–7937. [CrossRef]
356. Colmenares, J.C.; Luque, R. Heterogeneous photocatalytic nanomaterials: Prospects and challenges in selective transformations of biomass-derived compounds. *Chem. Soc. Rev.* **2014**, *43*, 765–778. [CrossRef] [PubMed]
357. Colón, G. Towards the hydrogen production by photocatalysis. *Appl. Catal. A Gen.* **2016**, *518*, 48–59. [CrossRef]
358. Fang, W.; Xing, M.; Zhang, J. Modifications on reduced titanium dioxide photocatalysts: A review. *J. Photochem. Photobiol. C Photochem. Rev.* **2017**, *32*, 21–39. [CrossRef]
359. Fornasiero, P.; Christoforidis, K.C. Photocatalytic Hydrogen production: A rift into the future energy supply. *ChemCatChem* **2017**, *9*, 1523–1544.
360. Fresno, F.; Portela, R.; Suárez, S.; Coronado, J.M. Photocatalytic materials: Recent achievements and near future trends. *J. Mater. Chem. A* **2014**, *2*, 2863–2884. [CrossRef]
361. Gholipour, M.R.; Dinh, C.-T.; Béland, F.; Do, T.-O. Nanocomposite heterojunctions as sunlight-driven photocatalysts for hydrogen production from water splitting. *Nanoscale* **2015**, *7*, 8187–8208. [CrossRef]
362. Grabowska, E. Selected perovskite oxides: Characterization, preparation and photocatalytic properties—A review. *Appl. Catal. B Environ.* **2016**, *186*, 97–126. [CrossRef]
363. Guo, L.; Jing, D.; Liu, M.; Chen, Y.; Shen, S.; Shi, J.; Zhang, K. Functionalized nanostructures for enhanced photocatalytic performance under solar light. *Beilstein J. Nanotechnol.* **2014**, *5*, 994–1004. [CrossRef]
364. Han, B.; Hu, Y.H. MoS_2 as a co-catalyst for photocatalytic hydrogen production from water. *Energy Sci. Eng.* **2016**, *4*, 285–304. [CrossRef]
365. Hisatomi, T.; Kubota, J.; Domen, K. Recent advances in semiconductors for photocatalytic and photoelectrochemical water splitting. *Chem. Soc. Rev.* **2014**, *43*, 7520–7535. [CrossRef] [PubMed]
366. Jiao, W.; Shen, W.; Rahman, Z.U.; Wang, D. Recent progress in red semiconductor photocatalysts for solar energy conversion and utilization. *Nanotechnol. Rev.* **2016**, *5*, 135–145. [CrossRef]
367. Junge, H.; Rockstroh, N.; Fischer, S.; Brückner, A.; Ludwig, R.; Lochbrunner, S.; Kühn, O.; Beller, M. Light to Hydrogen: Photocatalytic Hydrogen Generation from Water with Molecularly-Defined Iron Complexes. *Inorganics* **2017**, *5*, 14. [CrossRef]
368. Kagkoura, A.; Skaltsas, T.; Tagmatarchis, N. Transition metal chalcogenides/graphene ensembles for light-induced energy applications. *Chem. Eur. J.* **2017**, *23*, 12967–12979. [CrossRef]
369. Kitano, M.; Tsujimaru, K.; Anpo, M. Hydrogen production using highly active titanium oxide-based photocatalysts. *Top. Catal.* **2008**, *49*, 4. [CrossRef]
370. Kudo, A.; Miseki, Y. Heterogeneous photocatalyst materials for water splitting. *Chem. Soc. Rev.* **2009**, *38*, 253–278. [CrossRef]
371. Kumar, P.S.; Sundaramurthy, J.; Sundarrajan, S.; Babu, V.J.; Singh, G.; Allakhverdiev, S.I.; Ramakrishna, S. Hierarchical electrospun nanofibers for energy harvesting, production and environmental remediation. *Energy Environ. Sci.* **2014**, *7*, 3192–3222. [CrossRef]
372. Leung, D.Y.; Fu, X.; Wang, C.; Ni, M.; Leung, M.K.; Wang, X.; Fu, X. Hydrogen Production over Titania-Based Photocatalysts. *ChemSusChem* **2010**, *3*, 681–694. [CrossRef] [PubMed]
373. Li, C.; Xu, Y.; Tu, W.; Chen, G.; Xu, R. Metal-free photocatalysts for various applications in energy conversion and environmental purification. *Green Chem.* **2017**, *19*, 882–899. [CrossRef]

374. Francesco, P.; Fabrizio, S.; Marco, M.; Claudio, M.; Valter, M. The Role of Surface Texture on the Photocatalytic H_2Production on TiO_2. *Catalysts* **2019**, *9*, 32.
375. Zhang, X.; Wang, Y.; Liu, B.; Sang, Y.; Liu, H. Heterostructures construction on TiO_2 nanobelts: A powerful tool for building high-performance photocatalysts. *Appl. Catal. B Environ.* **2017**, *202*, 620–641. [CrossRef]
376. Li, X.; Yu, J.; Wageh, S.; Al-Ghamdi, A.A.; Xie, J. Graphene in photocatalysis: A review. *Small* **2016**, *12*, 6640–6696. [CrossRef] [PubMed]
377. Li, Y.; Li, Y.-L.; Sa, B.; Ahuja, R. Review of two-dimensional materials for photocatalytic water splitting from a theoretical perspective. *Catal. Sci. Technol.* **2017**, *7*, 545–559. [CrossRef]
378. Low, J.; Jiang, C.; Cheng, B.; Wageh, S.; Al-Ghamdi, A.A.; Yu, J. A Review of Direct Z-Scheme Photocatalysts. *Small Methods* **2017**, *1*, 1700080. [CrossRef]
379. Maeda, K. Photocatalytic water splitting using semiconductor particles: History and recent developments. *J. Photochem. Photobiol. C Photochem. Rev.* **2011**, *12*, 237–268. [CrossRef]
380. Martha, S.; Sahoo, P.C.; Parida, K. An overview on visible light responsive metal oxide based photocatalysts for hydrogen energy production. *RSC Adv.* **2015**, *5*, 61535–61553. [CrossRef]
381. Matsuoka, M.; Kitano, M.; Takeuchi, M.; Tsujimaru, K.; Anpo, M.; Thomas, J.M. Photocatalysis for new energy production: Recent advances in photocatalytic water splitting reactions for hydrogen production. *Catal. Today* **2007**, *122*, 51–61. [CrossRef]
382. Morales-Torres, S.; Pastrana-Martínez, L.M.; Figueiredo, J.L.; Faria, J.L.; Silva, A.M. Design of graphene-based TiO_2 photocatalysts—A review. *Environ. Sci. Pollut. Res.* **2012**, *19*, 3676–3687. [CrossRef] [PubMed]
383. Nguyen-Phan, T.-D.; Baber, A.E.; Rodriguez, J.A.; Senanayake, S.D. Au and Pt nanoparticle supported catalysts tailored for H_2 production: From models to powder catalysts. *Appl. Catal. A Gen.* **2016**, *518*, 18–47. [CrossRef]
384. Ni, M.; Leung, M.K.; Leung, D.Y.; Sumathy, K. A review and recent developments in photocatalytic water-splitting using TiO_2 for hydrogen production. *Renew. Sustain. Energy Rev.* **2007**, *11*, 401–425. [CrossRef]
385. Nurlaela, E.; Ziani, A.; Takanabe, K. Tantalum nitride for photocatalytic water splitting: Concept and applications. *Mater. Renew. Sustain. Energy* **2016**, *5*, 18. [CrossRef]
386. Pasternak, S.; Paz, Y. On the similarity and dissimilarity between photocatalytic water splitting and photocatalytic degradation of pollutants. *ChemPhysChem* **2013**, *14*, 2059–2070. [CrossRef]
387. Preethi, V.; Kanmani, S. Photocatalytic hydrogen production. *Mater. Sci. Semicond. Process.* **2013**, *16*, 561–575. [CrossRef]
388. Primo, A.; Corma, A.; García, H. Titania supported gold nanoparticles as photocatalyst. *Phys. Chem. Chem. Phys.* **2011**, *13*, 886–910. [CrossRef]
389. Protti, S.; Albini, A.; Serpone, N. Photocatalytic generation of solar fuels from the reduction of H_2O and CO_2: A look at the patent literature. *Phys. Chem. Chem. Phys.* **2014**, *16*, 19790–19827. [CrossRef]
390. Puga, A.V. Photocatalytic production of hydrogen from biomass-derived feedstocks. *Coord. Chem. Rev.* **2016**, *315*, 1–66. [CrossRef]
391. Ran, J.; Zhang, J.; Yu, J.; Jaroniec, M.; Qiao, S.Z. Earth-abundant cocatalysts for semiconductor-based photocatalytic water splitting. *Chem. Soc. Rev.* **2014**, *43*, 7787–7812. [CrossRef]
392. Samokhvalov, A. Hydrogen by photocatalysis with nitrogen codoped titanium dioxide. *Renew. Sustain. Energy Rev.* **2017**, *72*, 981–1000. [CrossRef]
393. Serrano, D.P.; Coronado, J.M.; Víctor, A.; Pizarro, P.; Botas, J.Á. Advances in the design of ordered mesoporous materials for low-carbon catalytic hydrogen production. *J. Mater. Chem. A* **2013**, *1*, 12016–12027. [CrossRef]
394. Sharma, P.; Kolhe, M.L. Review of sustainable solar hydrogen production using photon fuel on artificial leaf. *Int. J. Hydrogen Energy* **2017**, *42*, 22704–22712. [CrossRef]
395. Shi, J.; Guo, L. ABO_3-based photocatalysts for water splitting. *Prog. Nat. Sci. Mater. Int.* **2012**, *22*, 592–615. [CrossRef]
396. Shimura, K.; Yoshida, H. Heterogeneous photocatalytic hydrogen production from water and biomass derivatives. *Energy Environ. Sci.* **2011**, *4*, 2467–2481. [CrossRef]
397. Stroyuk, A.; Kryukov, A.; Kuchmii, S.Y.; Pokhodenko, V. Semiconductor photocatalytic systems for the production of hydrogen by the action of visible light. *Theor. Exp. Chem.* **2009**, *45*, 209. [CrossRef]
398. Wang, H.; Yuan, X.; Wu, Y.; Huang, H.; Peng, X.; Zeng, G.; Zhong, H.; Liang, J.; Ren, M. Graphene-based materials: Fabrication, characterization and application for the decontamination of wastewater and wastegas and hydrogen storage/generation. *Adv. Colloid Interface Sci.* **2013**, *195*, 19–40. [CrossRef]

399. Wang, H.; Zhang, L.; Chen, Z.; Hu, J.; Li, S.; Wang, Z.; Liu, J.; Wang, X. Semiconductor heterojunction photocatalysts: Design, construction, and photocatalytic performances. *Chem. Soc. Rev.* **2014**, *43*, 5234–5244. [CrossRef]
400. Wang, L. Strategies for efficient solar water splitting using carbon nitride. *Chem. Asian J.* **2017**, *12*, 1421–1434.
401. Wang, M.; Han, K.; Zhang, S.; Sun, L. Integration of organometallic complexes with semiconductors and other nanomaterials for photocatalytic H_2 production. *Coord. Chem. Rev.* **2015**, *287*, 1–14. [CrossRef]
402. Watanabe, M. Dye-sensitized photocatalyst for effective water splitting catalyst. *Sci. Technol. Adv. Mater.* **2017**, *18*, 705–723. [CrossRef]
403. Wen, M.; Mori, K.; Kuwahara, Y.; An, T.; Yamashita, H. Design and architecture of metal organic frameworks for visible light enhanced hydrogen production. *Appl. Catal. B Environ.* **2017**, *218*, 555–569. [CrossRef]
404. Xiao, F.X.; Miao, J.; Tao, H.B.; Hung, S.F.; Wang, H.Y.; Yang, H.B.; Chen, J.; Chen, R.; Liu, B. One-Dimensional Hybrid Nanostructures for Heterogeneous Photocatalysis and Photoelectrocatalysis. *Small* **2015**, *11*, 2115–2131. [CrossRef]
405. Xie, G.; Zhang, K.; Guo, B.; Liu, Q.; Fang, L.; Gong, J.R. Graphene-Based Materials for Hydrogen Generation from Light-Driven Water Splitting. *Adv. Mater.* **2013**, *25*, 3820–3839. [CrossRef]
406. Xing, J.; Fang, W.Q.; Zhao, H.J.; Yang, H.G. Inorganic photocatalysts for overall water splitting. *Chem. Asian J.* **2012**, *7*, 642–657. [CrossRef]
407. Xu, Y.; Xu, R. Nickel-based cocatalysts for photocatalytic hydrogen production. *Appl. Surf. Sci.* **2015**, *351*, 779–793. [CrossRef]
408. Xu, Y.; Zhang, B. Hydrogen photogeneration from water on the biomimetic hybrid artificial photocatalytic systems of semiconductors and earth-abundant metal complexes: Progress and challenges. *Catal. Sci. Technol.* **2015**, *5*, 3084–3096. [CrossRef]
409. Ye, S.; Wang, R.; Wu, M.-Z.; Yuan, Y.-P. A review on gC_3N_4 for photocatalytic water splitting and CO_2 reduction. *Appl. Surf. Sci.* **2015**, *358*, 15–27. [CrossRef]
410. Yin, S.; Han, J.; Zhou, T.; Xu, R. Recent progress in gC_3N_4 based low cost photocatalytic system: Activity enhancement and emerging applications. *Catal. Sci. Technol.* **2015**, *5*, 5048–5061. [CrossRef]
411. Yuan, Y.J.; Lu, H.W.; Yu, Z.T.; Zou, Z.G. Noble-Metal-Free Molybdenum Disulfide Cocatalyst for Photocatalytic Hydrogen Production. *ChemSusChem* **2015**, *8*, 4113–4127. [CrossRef]
412. Zhang, P.; Zhang, J.; Gong, J. Tantalum-based semiconductors for solar water splitting. *Chem. Soc. Rev.* **2014**, *43*, 4395–4422. [CrossRef]
413. Zhang, Q.; Gangadharan, D.T.; Liu, Y.; Xu, Z.; Chaker, M.; Ma, D. Recent advancements in plasmon-enhanced visible light-driven water splitting. *J. Mater.* **2017**, *3*, 33–50. [CrossRef]
414. Zhang, X.; Peng, T.; Song, S. Recent advances in dye-sensitized semiconductor systems for photocatalytic hydrogen production. *J. Mater. Chem. A* **2016**, *4*, 2365–2402. [CrossRef]
415. Zhao, X.; Wang, P.; Long, M. Electro- and Photocatalytic Hydrogen Production by Molecular Cobalt Complexes with Pentadentate Ligands. *Comments Inorg. Chem.* **2017**, *37*, 238–270. [CrossRef]
416. Zhao, Z.; Sun, Y.; Dong, F. Graphitic carbon nitride based nanocomposites: A review. *Nanoscale* **2015**, *7*, 15–37. [CrossRef] [PubMed]
417. Zou, X.; Zhang, Y. Noble metal-free hydrogen evolution catalysts for water splitting. *Chem. Soc. Rev.* **2015**, *44*, 5148–5180. [CrossRef] [PubMed]
418. Shwetharani, R.; Sakar, M.; Fernando, C.; Binas, V.; Balakrishna, R.G. Recent advances and strategies to tailor the energy levels, active sites and electron mobility in titania and its doped/composite analogues for hydrogen evolution in sunlight. *Catal. Sci. Technol.* **2019**, *9*, 12–46. [CrossRef]
419. Yuan, Y.-J.; Chen, D.; Yu, Z.-T.; Zou, Z.-G. Cadmium sulfide-based nanomaterials for photocatalytic hydrogen production. *J. Mater. Chem. A* **2018**, *6*, 11606–11630. [CrossRef]
420. Yuan, Y.-J.; Ye, Z.-J.; Lu, H.-W.; Hu, B.; Li, Y.-H.; Chen, D.-Q.; Zhong, J.-S.; Yu, Z.-T.; Zou, Z.-G. Constructing anatase TiO_2 nanosheets with exposed (001) facets/layered MoS_2 two-dimensional nanojunctions for enhanced solar hydrogen generation. *ACS Catal.* **2015**, *6*, 532–541. [CrossRef]
421. Liu, S.-H.; Tang, W.-T.; Lin, W.-X. Self-assembled ionic liquid synthesis of nitrogen-doped mesoporous TiO_2 for visible-light-responsive hydrogen production. *Int. J. Hydrogen Energy* **2017**, *42*, 24006–24013. [CrossRef]
422. Chen, Z.; Jiang, X.; Zhu, C.; Shi, C. Chromium-modified $Bi_4Ti_3O_{12}$ photocatalyst: Application for hydrogen evolution and pollutant degradation. *Appl. Catal. B Environ.* **2016**, *199*, 241–251. [CrossRef]

423. Yang, S.; Wang, H.; Yu, H.; Zhang, S.; Fang, Y.; Zhang, S.; Peng, F. A facile fabrication of hierarchical Ag nanoparticles-decorated N-TiO_2 with enhanced photocatalytic hydrogen production under solar light. *Int. J. Hydrogen Energy* **2016**, *41*, 3446–3455. [CrossRef]
424. Silva, L.A.; Ryu, S.Y.; Choi, J.; Choi, W.; Hoffmann, M.R. Photocatalytic hydrogen production with visible light over Pt-interlinked hybrid composites of cubic-phase and hexagonal-phase CdS. *J. Phys. Chem. C* **2008**, *112*, 12069–12073. [CrossRef]
425. Qin, N.; Xiong, J.; Liang, R.; Liu, Y.; Zhang, S.; Li, Y.; Li, Z.; Wu, L. Highly efficient photocatalytic H_2 evolution over MoS_2/CdS-TiO_2 nanofibers prepared by an electrospinning mediated photodeposition method. *Appl. Catal. B Environ.* **2017**, *202*, 374–380. [CrossRef]
426. Gopannagari, M.; Kumar, D.P.; Reddy, D.A.; Hong, S.; Song, M.I.; Kim, T.K. In situ preparation of few-layered WS_2 nanosheets and exfoliation into bilayers on CdS nanorods for ultrafast charge carrier migrations toward enhanced photocatalytic hydrogen production. *J. Catal.* **2017**, *351*, 153–160. [CrossRef]
427. Wang, M.; Na, Y.; Gorlov, M.; Sun, L. Light-driven hydrogen production catalysed by transition metal complexes in homogeneous systems. *Dalton Trans.* **2009**, 6458–6467. [CrossRef] [PubMed]
428. Linkous, C.A.; Huang, C.; Fowler, J.R. UV photochemical oxidation of aqueous sodium sulfide to produce hydrogen and sulfur. *J. Photochem. Photobiol. A Chem.* **2004**, *168*, 153–160. [CrossRef]
429. Huang, C.; Linkous, C.A.; Adebiyi, O.; T-Raissi, A. Hydrogen production via photolytic oxidation of aqueous sodium sulfite solutions. *Environ. Sci. Technol.* **2010**, *44*, 5283–5288. [CrossRef]
430. Li, C.; Hu, P.; Meng, H.; Jiang, Z. Role of Sulfites in the Water Splitting Reaction. *J. Solut. Chem.* **2016**, *45*, 67–80. [CrossRef]
431. Husin, H.; Adisalamun, S.Y.; Asnawi, T.M.; Hasfita, F. Pt nanoparticle on $La_{0.02}Na_{0.98}TaO_3$ catalyst for hydrogen evolution from glycerol aqueous solution. *AIP Conf. Proc.* **2017**, *1788*, 030073.
432. López-Tenllado, F.; Hidalgo-Carrillo, J.; Montes, V.; Marinas, A.; Urbano, F.; Marinas, J.; Ilieva, L.; Tabakova, T.; Reid, F. A comparative study of hydrogen photocatalytic production from glycerol and propan-2-ol on M/TiO_2 systems (M = Au, Pt, Pd). *Catal. Today* **2017**, *280*, 58–64. [CrossRef]
433. Li, F.; Gu, Q.; Niu, Y.; Wang, R.; Tong, Y.; Zhu, S.; Zhang, H.; Zhang, Z.; Wang, X. Hydrogen evolution from aqueous-phase photocatalytic reforming of ethylene glycol over Pt/TiO_2 catalysts: Role of Pt and product distribution. *Appl. Surf. Sci.* **2017**, *391*, 251–258. [CrossRef]
434. Oscar, Q.C.; Socorro, O.R.; Solís-Gómezb, A.; Rosendo, L.; Ricardo, G. Enhanced photocatalytic hydrogen production by CdS nanofibers modified with graphene oxide and nickel nanoparticles under visible light. *Fuel* **2019**, *237*, 227–235.
435. Andrea, S.; Francesca, G.; Federica, M.; Michela, S.; Daniele, D.; Lorenzo, M.; Antonella, P. Photocatalytic hydrogen evolution assisted by aqueous (waste)biomass under simulated solar light: Oxidized g-C_3N_4 vs. P25 titanium dioxide. *Int. J. Hydrogen Energy* **2019**, *44*, 4072–4078.
436. Tao, C.; Jie, M.; Qingyun, L.; Xiao, W.; Jixue, L.; Ze, Z. One-step synthesis of hollow $BaZrO_3$ nanocrystals with oxygen vacancies for photocatalytic hydrogen evolution from pure water. *J. Alloys Compd.* **2019**, *780*, 498–503.
437. Bahruji, H.; Bowker, M.; Davies, P.R.; Pedrono, F. New insights into the mechanism of photocatalytic reforming on Pd/TiO_2. *Appl. Catal. B Environ.* **2011**, *107*, 205–209. [CrossRef]
438. Fu, X.; Wang, X.; Leung, D.Y.; Gu, Q.; Chen, S.; Huang, H. Photocatalytic reforming of C_3-polyols for H_2 production: Part (I). Role of their OH groups. *Appl. Catal. B Environ.* **2011**, *106*, 681–688. [CrossRef]
439. Shkrob, I.A.; Sauer, M.C.; Gosztola, D. Efficient, rapid photooxidation of chemisorbed polyhydroxyl alcohols and carbohydrates by TiO_2 nanoparticles in an aqueous solution. *J. Phys. Chem. B* **2004**, *108*, 12512–12517. [CrossRef]
440. Shkrob, I.A.; Sauer, M.C. Hole Scavenging and Photo-Stimulated Recombination of Electron—Hole Pairs in Aqueous TiO_2 Nanoparticles. *J. Phys. Chem. B* **2004**, *108*, 12497–12511. [CrossRef]
441. Du, M.-H.; Feng, J.; Zhang, S. Photo-oxidation of polyhydroxyl molecules on TiO_2 surfaces: From hole scavenging to light-induced self-assembly of TiO_2-cyclodextrin wires. *Phys. Rev. Lett.* **2007**, *98*, 066102. [CrossRef]
442. Wang, B.; Zhang, J.; Huang, F. Enhanced visible light photocatalytic H_2 evolution of metal-free g-C_3N_4/SiC heterostructured photocatalysts. *Appl. Surf. Sci.* **2017**, *391*, 449–456. [CrossRef]

443. Zhang, Z.; Zhang, Y.; Lu, L.; Si, Y.; Zhang, S.; Chen, Y.; Dai, K.; Duan, P.; Duan, L.; Liu, J. Graphitic carbon nitride nanosheet for photocatalytic hydrogen production: The impact of morphology and element composition. *Appl. Surf. Sci.* **2017**, *391*, 369–375. [CrossRef]
444. Fang, L.J.; Wang, X.L.; Li, Y.H.; Liu, P.F.; Wang, Y.L.; Zeng, H.D.; Yang, H.G. Nickel nanoparticles coated with graphene layers as efficient co-catalyst for photocatalytic hydrogen evolution. *Appl. Catal. B Environ.* **2017**, *200*, 578–584. [CrossRef]
445. Yuan, Y.J.; Shen, Z.; Wu, S.; Su, Y.; Pei, L.; Ji, Z.; Ding, M.; Bai, W.; Chen, Y.; Yu, Z.T.; et al. Liquid exfoliation of g-C_3N_4 nanosheets to construct 2D-2D MoS_2/g-C_3N_4 photocatalyst for enhanced photocatalytic H_2 production activity. *Appl. Catal. B Environ.* **2019**, *246*, 120–128. [CrossRef]
446. Cai, J.; Shen, J.; Zhang, X.; Ng, Y.H.; Huang, J.; Guo, W.; Lin, C.; Lai, Y. Light-Driven Sustainable Hydrogen Production Utilizing TiO_2 Nanostructures: A Review. *Small* **2019**, *3*, 1800184. [CrossRef]
447. Wang, C.; Wang, L.; Jin, J.; Liu, J.; Li, Y.; Wu, M.; Chen, L.; Wang, B.; Yang, X.; Su, B.-L. Probing effective photocorrosion inhibition and highly improved photocatalytic hydrogen production on monodisperse PANI@ CdS core-shell nanospheres. *Appl. Catal. B Environ.* **2016**, *188*, 351–359. [CrossRef]
448. Song, J.; Zhao, H.; Sun, R.; Li, X.; Sun, D. An efficient hydrogen evolution catalyst composed of palladium phosphorous sulphide (PdP ~ 0.33 S ~ 1.67) and twin nanocrystal $Zn_{0.5}Cd_{0.5}S$ solid solution with both homo-and hetero-junctions. *Energy Environ. Sci.* **2017**, *10*, 225–235. [CrossRef]
449. Ma, S.; Xie, J.; Wen, J.; He, K.; Li, X.; Liu, W.; Zhang, X. Constructing 2D layered hybrid CdS nanosheets/MoS_2 heterojunctions for enhanced visible-light photocatalytic H_2 generation. *Appl. Surf. Sci.* **2017**, *391*, 580–591. [CrossRef]
450. Cheng, F.; Yin, H.; Xiang, Q. Low-temperature solid-state preparation of ternary CdS/g-C_3N_4/CuS nanocomposites for enhanced visible-light photocatalytic H_2-production activity. *Appl. Surf. Sci.* **2017**, *391*, 432–439. [CrossRef]
451. Tian, F.; Hou, D.; Hu, F.; Xie, K.; Qiao, X.; Li, D. Pouous TiO_2 nanofibers decorated CdS nanoparticles by SILAR method for enhanced visible-light-driven photocatalytic activity. *Appl. Surf. Sci.* **2017**, *391*, 295–302. [CrossRef]
452. Vignesh, K.; Suganthi, A.; Min, B.-K.; Kang, M. Photocatalytic activity of magnetically recoverable $MnFe_2O_4$/g-C_3N_4/TiO_2 nanocomposite under simulated solar light irradiation. *J. Mol. Catal. A Chem.* **2014**, *395*, 373–383. [CrossRef]
453. Zhen, W.; Ning, X.; Yang, B.; Wu, Y.; Li, Z.; Lu, G. The enhancement of CdS photocatalytic activity for water splitting via anti-photocorrosion by coating Ni_2P shell and removing nascent formed oxygen with artificial gill. *Appl. Catal. B Environ.* **2018**, *221*, 243–257. [CrossRef]